TRIBHUVAN UNIVERSITY

INSTITUTE OF ENGINEERING

PULCHOWK CAMPUS

THESIS NO. 079/MSCCD/018

Ranking and Evaluation of CMIP6 Climate Models Using Extreme Climate Indices: A Study in the Mid-Hills of Central Nepal

by

Susmita Khanal

(079MSCCD018)

A THESIS

SUBMITTED TO THE DEPARTMENT OF APPLIED SCIENCES AND CHEMICAL ENGINEERING IN PARTIAL FULFILLMENT OF THE REQUIREMENTS FOR THE DEGREE OF MASTER IN CLIMATE CHANGE AND DEVELOPMENT

DEPARTMENT OF APPLIED SCIENCES AND CHEMICAL ENGINEERING

LALITPUR, NEPAL

May, 2025

COPYRIGHT

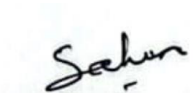

Pro. Dr. Sahira Joshi

Head

Department of Applied Sciences and Chemical Engineering

Pulchowk Campus, Institute of Engineering

Pulchowk, Lalitpur

Nepal

TRIBHUVAN UNIVERSITY

INSTITUTE OF ENGINEERING

PULCHOWK CAMPUS

DEPARTMENT OF APPLIED SCIENCES AND CHEMICAL ENGINEERING

The thesis titled **"Ranking and Evaluation of CMIP6 Climate Models Using Extreme Climate Indices: A study in the Mid-Hills of Central Nepal"** prepared and submitted by Susmita Khanal in partial fulfilment of the requirements for the degree of Master of Science (M.Sc.) in Climate Change and Development has been examined by us and is accepted for the award of M. Sc. in Climate Change and Development by Tribhuvan University.

The undersigned certify that they have read, and recommended to the Institute of Engineering for acceptance, a thesis report entitled **"Ranking and Evaluation of CMIP6 Climate Models Using Extreme Climate Indices: A study in the Mid-Hills of Central Nepal"** submitted by Susmita Khanal in partial fulfillment of the requirements for the degree of Master in Climate Change and Development

Supervisor:

Asst. Prof. Dr. Babu Ram Tiwari

Department of Applied Sciences and Chemical Engineering,

Pulchowk Campus

External Examiner:

Asso. Prof. Dr. Dhiraj Pradhananga

Department of Meteorology

Tri Chandra Multiple Campus

Program Coordinator:

Prof. Dr. Rinita Rajbhadari

Climate Change and Development Program

Department of Applied Sciences and Chemical Engineering

Head of Department:

Prof. Dr. Sahira Joshi

Department of Applied Sciences and Chemical Engineering

Pulchowk Campus

Date: May,2025

DECLARATION

I hereby declare that this study titled **"Ranking and Evaluation of CMIP6 Climate Models Using Extreme Climate Indices: A study in the Mid-Hills of Central Nepal "**is based on my original research work. Related works on the topic by other researchers have been duly acknowledged. I owe all the liabilities relating to the accuracy and authenticity of the data and any other information included hereunder.

Susmita Khanal

079MSCCD018

MSc in Climate Change and Development

Date: May,2025

ACKNOWLEDGEMENTS

I would like to express my profound gratitude to Professor Dr. Rinita Rajbhandari, our coordinator of Climate Change and Development, for offering us the opportunity to explore diverse concepts within the field climate change.

I would like to express my sincere gratitude to the Department of Hydrology and Meteorology (DHM), Nepal, for providing the observed climate data used in this study, despite its limitations. I also appreciate the CMIP6 modeling groups for making their datasets publicly accessible, which contributed to the analysis.

Special thanks go to my supervisor Assistant Professor Dr. Babu Ram Tiwari for his valuable guidance, constructive feedback and continuous support throughout this research. His insights have been instrumental in shaping this study. I am also grateful to my colleagues and affiliated institution for their assistance, resources and encouragement during the research process.

Similarly, I would like to thank everyone who offered direct and indirect assistance in this work.

ABSTRACT

Climate change has led to an increase in extreme weather events, significantly impacting ecosystems, infrastructure and public health. General Circulation Models play a crucial role in predicting climate variability and supporting adaptation strategies. However, their performance varies across different regions and climate variables, necessitating model evaluation before application in impact assessments. This study assesses the effectiveness of selected CMIP6 GCMs—ACCESS-ESM1.5, EC-EARTH3-VEG, INM-CM4.8, MIROC6, MPI-ESM1.2-LR, MRI-ESM2.0 and NESM3 in simulating precipitation-based climate extreme indices in mid hills of central Nepal. The study employs observed climate data from meteorological stations to evaluate the models based on statistical performance metrics, including Correlation Coefficient, Normalized Root Mean Square Deviation, Absolute Normalized Root Mean Square Deviation and Average Absolute Relative Deviation. Additionally, the models were ranked using an entropy-weighted decision-making approach to determine their suitability in representing extreme climate indices such as Consecutive Dry Days, Consecutive Wet Days and Heavy Precipitation Days. the analysis revealed that no single model consistently outperformed across all indices and locations. However, MIROC6 demonstrated the most stable performance overall. EC-EARTH3-VEG performed best for CDD, NESM3 and MIROC6 for CWD, and ACCESS-ESM-1.5 for R10, although the latter showed poor performance for the other indices. The findings suggest that while the evaluated CMIP6 models are useful for climate studies in the Central Hill Region, careful selection based on specific indices and local conditions is necessary. The study recommends adopting a multi-model ensemble approach to reduce uncertainties. Limitations include the use of only three meteorological stations, a focus on three precipitation indices, and reliance solely on historical simulations. Future research should incorporate multiple SSP-RCP scenarios, expand the spatial and temporal observational dataset, and include a wider range of extreme climate indices. The results have important policy implications for climate change adaptation, water resource management, and disaster risk reduction strategies in Nepal's mid-hill regions.

Keywords: Climate Variability, Performance Indicator, Model Intercomparison

TABLE OF CONTENTS

LIST OF FIGURES

LIST OF TABLES

ABBREVIATIONS AND ACRONYMS

AARD	Average Absolute Relative Deviation
ANRMSD	Absolute Normalized Root Mean Square Deviation
CMIP	Coupled Model Intercomparison Project
CC	Correlation Coefficient
CDD	Consecutive Dry Days
CWD	Consecutive Wet Days
DHM	Department of Hydrology and Meteorology
ETCDDI	Expert Team on Climate Change Detection and Indices
FD	Frost Days
GCMs	General Circulation Models
IPCC	Intergovernmental Panel on Climate Change
MME	Multi Model Ensemble
NRMSD	Normalized Root Mean Square Deviation
PRCP	Precipitation
QM	Quantile Mapping
RCP	Representative Concentration Pathways
RMSE	Root Mean Square Error
SPA	Shared Climate Policy Assumptions
SSP	Shared Socio-economic Pathways
WCRP	World Climate Research Program
WGCM	Working Group on Coupled Modelling

1 INTRODUCTION

1.1 Background

Shifts in precipitation patterns across the globe have raised concerns due to their influence on water availability, ecosystem health and the increasing frequency of extreme weather events (Daramola & Xu, 2022). Since the 1950s, extreme weather and climate events associated with human-induced climate change have become more frequent and intense worldwide (IPCC, 2021). The rising levels of greenhouse gases in the atmosphere, mainly from human activities, have significantly altered climate patterns. This has led to global warming, sea-level rise and more frequent and intense extreme weather events. These changes present serious threats to ecosystems, infrastructure, food security and public health, requiring strong scientific methods to understand, predict and mitigate their effects (IPCC, 2007). Furthermore, in Himalayan countries like Nepal, climate change is a critical factor influencing sustainability in the region. The rising temperatures and shifting weather patterns have accelerated glacier melt, increased the frequency of extreme weather events and heightened the risk of natural disasters such as floods and landslides. These changes pose significant threats to the livelihoods, food security and health of millions of people living in these areas (Pradhan et al., 2021). Therefore, it is essential to gain a deeper understanding of extreme value behaviors, particularly to comprehend their sectoral impacts and to devise effective adaptation strategies)ETCCDI, 2009(.

Climate models are essential for predicting future climate patterns by simulating the Earth's climate system based on physical laws and empirical relationships (Baghel et al., 2022). These models integrate various components such as land surface, ocean and atmosphere to create a comprehensive picture of climate dynamics (Eyring et al., 2016). The coupled Model Intercomparison Project (CMIP) represent a significant global initiative aimed at understanding climate changes over time. CMIP6 involving international and regional organizations, has developed and refined multiple climate models to better comprehend past, present and future climate conditions (Eyring et al., 2016; Srivastava et al., 2020; Riahi et al., 2017). Climate models operates based on numerous assumptions, initial boundary conditions, model formation ,resolution and complexity, observational uncertainty and parametric and structural uncertainty (Palmer, 2000; Pathak et al., 2023; Webster & Sokolov, 1998). To address these uncertainties, ensemble forecasting methods are used, which involve running multiple models with different initial conditions and parameters to generate a

range of possible outcomes. This approach can provide probabilistic predictions that better capture the uncertainty in climate forecasts (Palmer, 2000).

Evaluating General Circulation Models (GCMs) is essential before their application in climate change studies, as their performance can differ greatly by region and specific model (IPCC, 2007). By examining the performance of GCMs, researchers can improve the simulation of various hydro-climatic variables, which may be critical for precise hydrological modeling. The key metrics used to evaluate the performance of General Circulation Models (GCMs) include Correlation Coefficient (CC), Normalized Root-Mean-Square Deviation (NRMSD), Absolute Normalized Root-Mean-Square Deviation (ANRMSD), Average Absolute Relative Deviation (AARD), Bias, Trend Comparison, Climate Indices (Altamirano del Carmen et al., 2021; Pradhan et al., 2021). These metrics provide a comprehensive assessment of GCM performance in simulating various climate variables and their characteristics, which is crucial for their application in climate change studies and hydrological modeling.

The primary aim of this research is to evaluate and rank climate models for different climate indices (CDD, CWD, R10) for mid hills of central Nepal

1.2 Research Gaps and Problem Statement

The rising frequency and severity of extreme weather events due to human-induced climate change pose major risks to ecosystems, infrastructure, food security and public health globally. In the Himalayas, these changes have hastened glacier melt and elevated the risk of natural disasters, threatening the livelihoods and well-being of millions (IPCC, 2021). Although accurate climate predictions are essential for developing effective adaptation strategies, the performance of existing climate models differs significantly across various regions and sectors, creating uncertainties in their use (Ren et al., 2020).

Despite the use of various climate models, such as general circulation models and regional climate models, to examine the impacts of climate change on Himalayan river basins (Dahal et al., 2020a) choosing the most suitable models remains a major challenge. The performance of GCMs varies widely by region and model, resulting in uncertainties in their application (Pradhan et al., 2021). Consequently, there is a crucial need to develop a robust methodology for evaluating and ranking climate models tailored to different sectors to improve the accuracy of climate predictions and support effective adaptation strategies (Baghel et al., 2022).

This research aims to fill the gap in current studies by creating and showcasing a methodology for assessing and ranking climate models specifically for the mid

hills of central Nepal which is part of the Central region of Nepal. By utilizing performance indicators and climate indices, the study seeks to pinpoint the most appropriate GCMs for simulating precipitation. The results will improve the reliability of climate forecasts and aid in the development of effective adaptation and mitigation strategies, offering a framework that can be extended to other river basins in the Himalayas.

1.3 Objectives

The study aims to access the performance of CMIP6 general circulation models in accurately simulating historical and projected precipitation based extreme indices in the Mid-Hills of central Nepal.

Specific Objectives:

- To select an appropriate GCMs for the basin.
- To evaluate the efficiency of GCMs in the selected study region.
- To rank the GCMs on the basis of performance indices for each selected climate indices among different stations and the study area.
- To provide recommendations for selecting the most reliable selected GCMs for each climate indices.

1.4 Scope

This research focuses on evaluating the ability of selected CMIP6 climate models to simulate precipitation extremes within the Seti Gandaki River Basin in Nepal. The assessment is based on observed rainfall data from three strategically located meteorological stations as station 804, station 808, and station 1004. These stations were selected for their reliable and long-term data records, as well as their geographic coverage of the basin.

The temporal scope covers the historical baseline period from 1980 to 2014, aligning with available observed precipitation data from the three meteorological stations in the Seti Gandaki Basin. Within this period, the study evaluates model performance using statistical indicators such as Correlation Coefficient, Normalized Root Mean Square Deviation, Absolute Normalized Root Mean Square Deviation, and Average Absolute Relative Deviation.

The analysis is limited to three precipitation-based climate indices: Consecutive Dry Days, Consecutive Wet Days, and Heavy Precipitation Days. These indices are particularly relevant for understanding rainfall variability and extremes, which

have direct implications for water resource management and disaster preparedness in the region.

This study does not extend to temperature variables or future climate projections. Its primary goal is to identify the most reliable models for simulating past precipitation extremes. The methodology and findings can serve as a foundation for future climate impact studies and model selection in similar river basins across the mid hills of central Nepal.

1.5 Limitations

The limitations of this study are as follows:

- The study focuses only on three stations, which, although spatially distributed, may not capture all the microclimatic variations in the basin.
- Only three precipitation-based climate indices were considered. Temperature-based indices and other socio-economic indicators were excluded.
- The performance of models was evaluated based on historical simulations. Future projections, particularly under different SSP-RCP scenarios, were not analyzed.

2 LITERATURE REVIEW

2.1 What Are Climate Models?

Climate models are complex computer programs the simulates the Earth's climate system. They are essential tools for understanding past, present and future. They also include variables like air pressure, temperature and wind. All of these are expressed as equations that a climate model must solve. Solving the equations produces a three-dimensional picture that shows natural climate patterns in action, like rainfall, ocean currents and the changing of seasons (climate portal). The evaluation of climate models is crucial for understanding their reliability in simulating weather patterns and informing water resource management (Sỳs et al., 2021). Simulation modeling is at the core of decision analysis methods for climate adaptation in the water sector (Borgomeo, 2022). These models enable learning about the complex behavior of river basins, testing of alternative adaptation decisions, exploration of uncertainties and navigation of trade-offs (Borgomeo, 2022). Modeling approaches are widely used to evaluate the impacts of climate change and assess the effectiveness of various adaptation measures like greenhouses, crop planting time shifts, managed aquifer recharge and improved irrigation technology (Zhao & Boll, 2022). In climate change impact studies, it's standard to use a group of global circulation model outputs to represent a broad spectrum of potential future climate scenarios (Seo et al., 2019).

The Coupled Model Intercomparison Project (CMIP), initiated by the Working Group on Coupled Modelling (WGCM) under the World Climate Research Programme, began two decades ago as an effort to compare a small number of early global climate models. These models conducted experiments using atmospheric models that were connected to a dynamic ocean, a basic land surface and thermodynamic sea ice (Meehl et al., 1997). CMIP aims to deepen our understanding of climate change, whether due to natural fluctuations or shifts in radiative forcings, by analyzing it through the lens of various climate models, covering the past, present and future. The growing significance and scope of CMIP have been a major success, but this very success brings challenges for everyone involved. As CMIP now includes more models, covering a broader array of processes and addressing a wider range of scientific questions, coordinating the project has become increasingly complicated. The rising interest in and demand for CMIP, driven by a growing number of scientific community's eager to explore diverse questions within climate science, has led to the project's expansion. This growth has resulted in a significant increase in the variety and volume of requested outputs from a growing number of experiments, placing considerable

strain on CMIP's technical infrastructure(Eyring et al., 2016a). The newest phase of the CMIP, called CMIP6, is anticipated to bring notable improvements over the previous phase, CMIP5. These advancements stem from better quantification of radiative forcing, accounting for both natural and human-induced influences, as well as the inclusion of aerosol effects, land use changes and other contributing factors (Gumus et al., 2023). To enhance the regional and local performance of global climate models, extensive research has been conducted on statistical downscaling, bias correction techniques and their applications in hydrometeorological impact studies. For processing CMIP6 GCM data in this study, the methods of quantile mapping, quantile delta mapping and detrended quantile mapping will be employed during the bias correction and downscaling stages(Gumus et al., 2023). The observed data such as precipitation(P), mean temperature(T), maximum temperature (Tx), minimum temperature (Tn) can be used as the observed data for the evaluation of climate models.

2.2 Global Scenarios: RCPs, SSPs and SPAs

Climate change is expected to have varied effects on both human and natural systems, with the severity and nature of these impacts differing by region, sector and over time. The scale of future consequences will be influenced by how the Earth system responds to changes in atmospheric composition, as well as by the success of mitigation and adaptation efforts in preventing, preparing for and managing these impacts. Additionally, development pathways, including shifts in demographics, economies, technologies and policies, will play a crucial role. Scenarios are used to examine and assess the wide-ranging uncertainties in these factors. A scenario provides a detailed outlook on the future of the human-climate system, encompassing both quantitative and qualitative aspects. In contrast, the term pathway refers to specific scenario elements, such as atmospheric concentration levels or development trends(Kebede et al., 2018a).

The use of scenario analysis as a strategic management tool to investigate potential future developments and their effects in order to facilitate adaptation decision-making in the face of uncertainty has long been recognized. In order to create self-consistent narratives or visions of the future, scenarios are logical, internally consistent and credible representations of potential paths of changing conditions based on "if, then" statements(Moss et al .,2010). In an environment of interacting complex systems and uncertainty, they are typically produced to explore the implications of long-term climate, environmental and anthropogenic futures for establishing strong policies. In an environment of interacting complex systems and uncertainty, they are typically produced to explore the implications

of long-term climate, environmental and anthropogenic futures for establishing strong policies(Harrison et al., 2015). The complexity of scenario representation arises from the several dimensions of change. Initially, scenarios in climate analysis placed a lot of emphasis on climate change and relatively little on other aspects (Hulme et al., 1999). Through the new global RCP–SSP–SPA scenario framework (Representative Concentration Pathways;(van Vuuren et al., 2011); Shared Socio-economic Pathways; (O'Neill et al., 2020a); and Shared climate Policy Assumptions; (Kriegler et al., 2014)), the Fifth Assessment Report (IPCC AR5) expands on this further to consider the climate, socio-economic and policy dimensions of change. Under various climate and socioeconomic scenarios, as well as with respect to adaptation and mitigation policy assumptions, the framework offers a basis for a better integrated assessment of the impacts of climate change and the need for adaption and mitigation. A climate-socio-economic-policy framework such as the RCP–SSP–SPA method has few full applications and application gets increasingly challenging as more dimensions are included (Kebede et al., 2018b).

2.3 CMIP6 Vs CMIP6: Advancement and Implications

The Coupled Model Intercomparison Project Phase 6 (CMIP6) represents a significant upgrade over CMIP5, offering improvements in scenario design, resolution, model physics, experimental structure, and data accessibility(Balaji et al., 2018; Eyring et al., 2016b; O'Neill et al., 2020b). One of the most fundamental changes is the replacement of Representative Concentration Pathways (RCPs) in CMIP5 with Shared Socioeconomic Pathways (SSPs) in CMIP6. While RCPs describe future radiative forcing trajectories(Van Vuuren et al., 2011), SSPs combine socioeconomic narratives with emission scenarios, enabling integrated assessments of climate change impacts and policy responses (O'Neill et al., 2020b). This facilitates a more nuanced exploration of how future societal choices may shape climate outcomes.

In terms of resolution, CMIP6 models offer enhanced horizontal and vertical resolutions compared to CMIP5, with many models achieving resolutions finer than 100 km, and some reaching as high as 25 km (Haarsma et al., 2016). This allows for a better representation of orographic effects, land-sea contrasts, and local climate variability, which is especially important for regions with complex terrain such as the Himalayas and river basins like the Seti Gandaki. High-resolution models are better suited for simulating localized phenomena including extreme rainfall, heatwaves, and monsoon dynamics (Roberts et al., 2018).

Significant progress has also been made in the physical representation of climate processes. CMIP6 models include improved schemes for cloud microphysics, aerosol-cloud interactions, convection, and land-surface processes, which contribute to more accurate simulations of the energy and hydrological cycles (Wehner et al., 2010). For example, updates in aerosol radiative forcing schemes have improved estimates of climate sensitivity and reduced long-standing biases in tropical precipitation (Myhre et al., 2017). These changes have resulted in a broader and more physically plausible range of equilibrium climate sensitivity (ECS) estimates in CMIP6 models(Zelinka et al., 2020).

CMIP6 also introduces a more modular and comprehensive experimental design. Unlike CMIP5, which followed a unified approach, CMIP6 is built around the DECK (Diagnostic, Evaluation and Characterization of Klima) experiments and a series of endorsed Model Intercomparison Projects (MIPs), each focusing on specific components or feedbacks of the climate system (Eyring et al., 2016). For instance, ScenarioMIP focuses on future emissions pathways under various SSPs, while HighResMIP investigates the role of horizontal resolution in simulating climate processes (Haarsma et al., 2016). This modular structure enables researchers to select specialized experiments tailored to their research needs, including the study of extreme events and regional climate change.

In addition, CMIP6 employs more accurate and consistent historical forcings, including updated records of volcanic aerosols, solar variability, and anthropogenic emissions(Hegerl et al., 2018). These improvements enhance the credibility of historical climate simulations, which are essential for evaluating model performance against observed extreme indices. Furthermore, the inclusion of advanced land-use datasets and anthropogenic land-cover changes improves the simulation of land-atmosphere feedbacks (Lawrence et al., 2016).

Finally, CMIP6 has made substantial improvements in data documentation, metadata standards, and version control. These enhancements ensure greater transparency, reproducibility, and accessibility of climate model outputs for the global research community (Balaji et al., 2018). Such improvements are particularly valuable for research involving multiple models and large datasets, such as this study, which evaluates CMIP6 model performance in reproducing extreme climate indices over the mid hills of central Nepal.

2.4 Climate Modelling in South Asia and the Himalayas

Recent advancements in climate modeling have significantly enhanced our understanding of climate dynamics in South Asia and the Himalayan region. The

Coupled Model Intercomparison Project Phase 6 has been instrumental in providing high-resolution climate projections, which are crucial for assessing regional climate variability and change (Bhuyan et al., 2024; Wijngaard et al., 2023). In Nepal, for instance, bias-corrected CMIP6 projections indicate a potential warming of 4–6°C and a 40–60% increase in precipitation by the end of the 21st century under high-emission scenarios, emphasizing the need for robust adaptation strategies(Dhital et al., 2023). Similarly, studies focusing on the Himalaya–Tibetan Highland have identified systematic biases in CMIP6 models, particularly cold and wet biases, but also highlight improvements in simulating spatial distributions of temperature and precipitation when using a subset of the best-performing models(Bhuyan et al., 2024). Furthermore, research utilizing variable-resolution Community Earth System Models has demonstrated improved simulations of cryosphere and hydrological variables in High Mountain Asia, which is vital for understanding water resource dynamics in the region (Wijngaard et al., 2023). These advancements underscore the importance of continuous model refinement and the integration of high-resolution data to better capture the complex climate processes in South Asia and the Himalayas.

2.5 Role of Bias Correction in Climate Modeling

Bias correction is an essential technique in climate modeling that addresses systematic errors in climate model outputs by aligning them more closely with observed data (Ehret et al., 2012; Maraun, 2016). Climate models, particularly GCMs, often misrepresent temperature and precipitation patterns due to coarse resolution and simplifications in representing physical processes(Teutschbein & Seibert, 2012) . These biases can significantly affect the accuracy of climate impact assessments, especially in regions with complex topography like the hilly region of central Nepal. Various statistical methods are employed to correct these biases. Traditional techniques include linear scaling and delta change, which correct the mean values but may not capture variability or extremes effectively (Teutschbein & Seibert, 2012). More advanced approaches such as quantile mapping (QM) and empirical quantile mapping (EQM) adjust the entire distribution of model outputs, offering better performance for extreme values(Gudmundsson et al., 2012) . Recent innovations like Q-GAM, a quantile-based generalized additive model, have shown improvements in precipitation correction (Lazoglou et al., 2024), while deep learning methods are being developed to preserve trends and handle multivariate relationships (Wang & Tian, 2024). These techniques enhance the realism of climate projections, making them more suitable for regional impact studies, but they rely on the assumption that historical relationships between

model output and observations will remain valid under future climate scenarios(Gao et al., 2024).

2.6 Climate extreme indices

An essential statistical tool for measuring and analyzing the frequency, length, intensity and occurrence of extreme weather and climatic events is the extreme climate indices. These indexes are essential for comprehending how the climate is changing, especially in light of global warming, which is increasing the frequency and intensity of extreme weather events including heatwaves, torrential downpours, droughts and cold snaps (Baghel et al., 2022a). The definition of an extreme and the threshold values for these extremes vary throughout nations. In an effort to create consistency, the ETCDDI has created 27 extreme climate indices that offer a thorough summary of the extremes in the climate and take into account all factors, not just the extreme. Percentile-based indices, such as TX90p -Warm Days and TX10p -Cold Days, are commonly used to quantify extreme climates. These indices indicate the proportion of days with daily maximum temperatures above the 90th and below the 10th percentile, respectively. Duration indices assess the maximum number of days with little or significant rainfall in a row. Examples of these indices include Consecutive Dry Days - CDD and Consecutive Wet Days - CWD. Threshold-based indices track days that surpass predetermined thresholds for precipitation or temperature, such as Frost Days - FD and Number of days with heavy precipitation - R10mm. Absolute indices that record the highest and lowest temperatures ever observed each year are called TXx (Max Tmax) and TNn (Min Tmin). These indices are frequently used in risk assessment to determine possible consequences on different sectors, in adaptation planning to guide policy decisions and strategies and in climate change research to evaluate trends in extreme weather occurrences. Scientists, decision-makers and interested parties can better comprehend and address the issues raised by extreme climate events by keeping an eye on these indexes.

2.7 Performance Statics

Performance metrics are essential for assessing the precision and dependability of predictive models, especially in domains like climate modeling. These metrics include Correlation Coefficient, Normalized Mean Root Square Deviation, Absolute Normalized Root Mean Square Deviation, Average Absolute Relative Deviation, Mean Squared Error and Root Mean Square Error (Pradhan et al., 2021). Values

near to 1 indicate a significant positive correlation. The Correlation Coefficient quantifies the direction and intensity of the linear relationship between observed and predicted values. By normalizing the Root Mean Square Deviation, NRMSD highlights how well a model predicts the observed values in relation to a reference. Like NRMSD, ANRMSD is concerned with the deviations of anomalies, or departures from a mean or baseline and it offers information on how well a model can represent changes from average circumstances. AARD provides a simple way to test the accuracy of a model by calculating the average of the absolute relative errors between the observed and predicted values. Higher performance is indicated by lower values. The mean square error penalizes greater errors more severely than the root mean square error, which is the square root of MSE and offers a measure of error size in the same units as the data. MSE and RMSE are closely related metrics. When combined, these statistics provide a thorough understanding of the model's performance, assisting in identifying areas in need of development and guaranteeing that forecasts are as precise and reliable.

2.8 Importance of Multi-Model Ensemble Approach

The multi-model ensemble approach has become a cornerstone in climate modeling due to its ability to incorporate a range of uncertainties and provide more robust climate projections (Dey et al., 2022; Kim et al., 2024). Individual climate models often produce varying outcomes due to differences in physical parameterizations, boundary conditions, and spatial resolution, leading to significant spread in projected climate variables (Manikanta et al., 2024). By combining outputs from multiple models, MMEs reduce the influence of individual model biases and provide a more reliable representation of future climate conditions (Kim et al., 2024). For example, (Kim et al., 2024) demonstrated that an MME approach improved the reliability of extreme rainfall projections over the Han River watershed by capturing higher-order statistical features. Similarly, (Dey et al., 2022) showed that integrating machine learning techniques such as support vector machines and random forests with MMEs in the Damodar River Basin led to superior performance in simulating both temperature and precipitation. However, the approach is not without limitations. (Manikanta et al., 2024) found that while CMIP6-based MMEs generally aligned well with observed data over India, they tended to underestimate certain precipitation indices, indicating that careful model evaluation and selection remain necessary. Despite such challenges, the MME approach significantly enhances the robustness of climate projections, especially for regional climate impact assessments and decision-making.

3 STUDY AREA

The focus of this study is central mid hilly region of Nepal, specially targeting area within the elevation range of 800 to 1000m above sea level. This mid hill zone represents a critical ecological and climatic transition between the lowland Terai plains and the high Himalayan regions. It is the part of Nepal's middle mountains, known for their complex topography, diverse climate and socio economic importance (DHM 2017, ICIMOD 2010).

Geographically, this elevation range spans several districts of Gandaki and Bagmati Provinces. The elevation range of 800–1000 m is typically classified as subtropical hill climate, experiencing warm summers, mild winters, and a distinct monsoon season from June to September.

Hydrologically, the area includes tributaries of the Gandaki river system, such as the Seti, Marshyangdi, and Kali Gandaki Rivers, which are essential for local livelihoods, agriculture, and hydropower generation (Neupane, 2022). The region is highly sensitive to climate variability and extremes, particularly due to its exposure to intense monsoonal rainfall, which can trigger landslides, flash floods, and soil erosion (Dahal et al., 2020).

Table 3-1 Location of study stations

Station	**Station No.**	**Latitude**	**Longitude**	**Elevation**	**Parameter**
Bandipur (Tanahun)	808	27.94183	84.40638	991m	Precipitation
Pokhara Airport (Kaski)	804	28.20018	83.97953	827m	Precipitation
Nuwakot (Nuwakot)	1004	27.91497	85.16464	966m	Precipitation

The selection of precipitation stations 804, 808 and 1004 was primarily based on their geographic coverage across the central mid hills and the availability of consistent and long-term rainfall data spanning 30 years, which is essential for climate trend analysis(WMO, 2021). According to the World Meteorological Organization (WMO), a minimum of 30 years of data is recommended for studying climate variables such as precipitation, temperature and humidity to ensure

reliable and representative assessments. The combination of broad spatial coverage and dependable data availability makes these stations well suited for analyzing precipitation patterns in the mid hills of central Nepal.

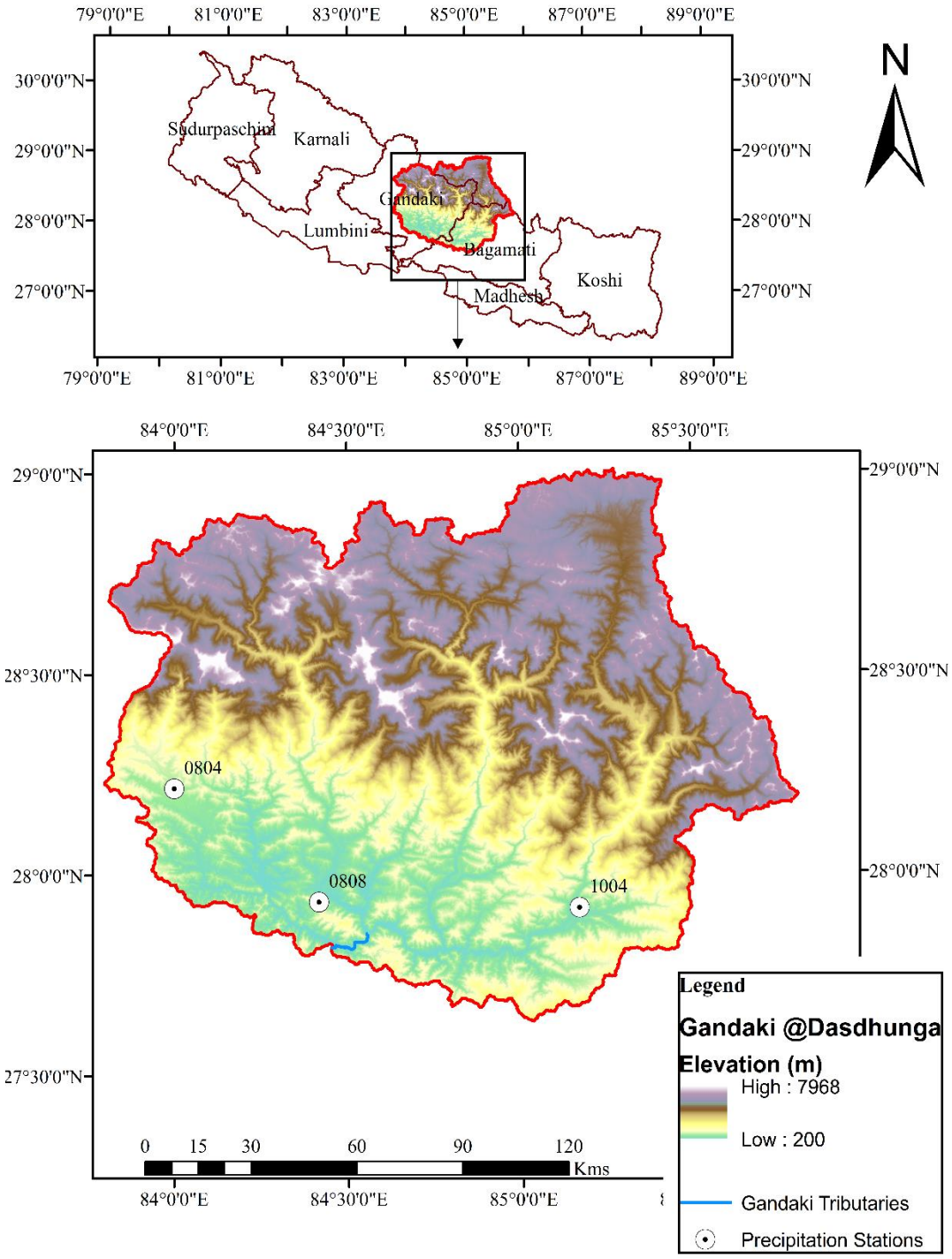

Figure 3-1 Location Map Of Study Area

This map illustrates the Seti Gandaki River watershed, focusing on its outlet point at Dasdhunga (27°47'28" N, 84°25'48" E) in central Nepal. The main map uses color shading to represent elevation, ranging from low-lying areas (200 meters)

in green to high-altitude mountain regions (up to 7968 meters) in shades of brown and white. This gradient clearly shows how the terrain rises sharply from the southern plains to the northern Himalayas. Such variation in elevation influences not only river flow and drainage patterns but also rainfall distribution and runoff behavior across the basin.

Blue lines trace the river networks, highlighting the courses of the Seti, Madi and Trishuli Rivers as they flow southward through the central hills of selected area. These rivers, fed by rainfall and snowmelt, are crucial sources of water for the downstream regions. Scattered throughout the map are precipitation monitoring stations, shown as white circles outlined in black and labeled as 804, 808, 1004. These stations are essential for collecting rainfall data.

In the top-right corner, an inset map places the watershed within the broader national context of Nepal.

4 DATA AND METHODOLOGY

4.1 Observed Data

The observed historical data on precipitation has been obtained from Department of Hydrology and Meteorology (DHM), Nepal. Thus obtained data are used to evaluate the climate models (Baghel et al., 2022a).

4.2 Climate Models Data

Over the last twenty years, the Intergovernmental Panel on Climate Change has produced various climate datasets, with the most recent being CMIP6 (Eyring et al., 2016). The outputs from multiple climate models have been gathered, stored and made publicly accessible to various communities and users. For this study, 7 GCMs were selected from the data set of CMIP6 consist of precipitation output from 1980 to 2014. These models were chosen based on a review of existing literature and research studies. The selection of the seven General Circulation Models (GCMs), ACCESS-ESM1.5, EC-EARTH3-VEG, INM-CM4.8, MIROC6, MPI-ESM1.2-LR, MRI-ESM2.0 and NESM3, from the CMIP6 data set was based on study done by (Mishra et al., 2020). According to (Mishra et al., 2020), several of these GCMs have been previously evaluated and found to effectively capture key climatic characteristics over the South Asian domain, including temperature and monsoonal precipitation trends. These models provide essential variables, precipitation and temperature, with continuous records from 1980 to 2014, aligning with the baseline period used in this study. Their relatively higher spatial resolutions also make them suitable for basin-scale climate assessments in complex terrains like the middle hilly regions of Nepal. Table 2 provides an overview of the models utilized, including their names, home institutions, resolutions and other key details.

Table 4-1 Summary of GCMs Used in This Study and Their Information Sources

S. N.	Model	Resolution (Lat. x Long.)	Institute	References
1	ACESS-ESM-1.5	1.25 x 1.875	Commonwealth Scientific and Industrial Research Organization (Australia)	(Dix et al., 2019)
2	EC-EARTH3-VEG	0.7 x 0.7	Swedish Meteorological and Hydrological Institute Norrkoping, Sweden	(Liu et al., 2022)
3	INM-CM4.8	2.0 x 1.5	Institute for Numerical Mathematics of Russian Academy of Sciences, Russia	(Volodin et al., 2018)
4	MIROC6	1.4 x 1.4	Atmosphere and Ocean Research Institute, University of Tokyo (Japan)	(Shiogama et al., 2019)
5	MPI-ESM1.2-LR	1.87 x 1.87	Max Plank Institute for Meteorology	(Wieners et al., 2019)
6	MRI- ESM2.0	1.12 x 1.13	Meteorological University of Information Tsukuba, Ibaraki, Japan	(Yukimoto et al., 2019)
7	NESM3	1.9 x1.9	Nanjing University of Information Science and Technology, China	(Baghel et al., 2022b)

4.3 Methodology

Figure 4-1 illustrates the overall methodological framework adopted in this study. The primary objective is to identify which of the seven selected CMIP6 GCMs best replicates the precipitation patterns in the mid hills of central Nepal under various climate extremes. To achieve this, the degree of agreement between GCM simulated data and observed station data was assessed using performance indicators. Specifically, four indicators—Correlation Coefficient, Normalized Root

Mean Square Deviation, Absolute Normalized Root Mean Square Deviation and Average Absolute Relative Deviation were selected based on their widespread application and relevance in recent literature. These indicators were chosen because they collectively provide a robust and balanced evaluation of model performance: CC captures the temporal correlation between simulated and observed trends(Gómez et al., 2023); NRMSD and ANRMSD quantify model error in a normalized, scale-independent manner (Gómez et al., 2023); and AARD offers a percentage-based measure of relative deviation, allowing for intuitive comparison across GCMs and indices (Hess et al., 2023). This combination ensures both the accuracy and consistency of model outputs are comprehensively assessed. Recent studies (Gómez et al., 2023; Hess et al., 2022) have emphasized the importance of using such multi-metric approaches for evaluating climate models, particularly when dealing with derived climate extremes. Accordingly, three precipitation-related extreme indices Consecutive Dry Days CDD, Consecutive Wet Days and Heavy Precipitation Days were selected from the ETCCDI list, based on their relevance to frequency, intensity and duration of precipitation extremes (Table 1). Using Python, these indices were computed for the period 1980–2014, both from GCM outputs and from ground-based station data and then evaluated using the selected indicators.

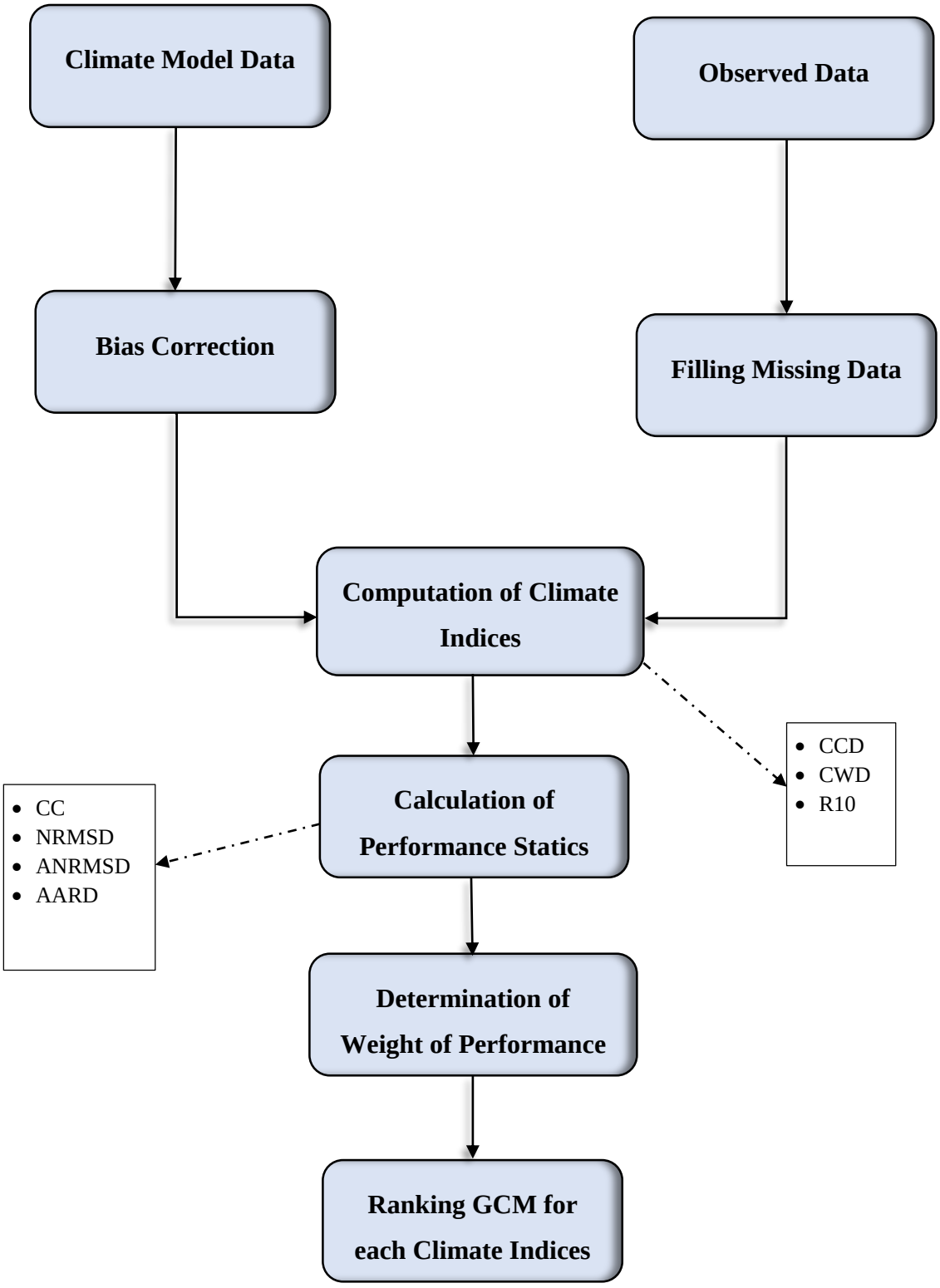

Figure 4-1 Methodological framework for this study

Step 1: First of all, the observed data of stations 804, 808, 1004 were taken from Department of Hydrology and Meteorology, Nepal. After that, climate data from climate model were extracted by using Python. With the help of observed data, bias correction was done for climate model. GCMs often exhibit systematic biases due to limitations in spatial resolution and simplifications in representing complex climate processes. These biases can lead to discrepancies between model outputs and observed data, particularly at regional or local scales. For instance, GCMs may overestimate or underestimate precipitation and temperature extremes, affecting the reliability of climate projections used in impact assessments and decision-making processes(Shrestha et al., 2017).

To address these discrepancies, bias correction methods are employed to adjust GCM outputs, enhancing their alignment with observed data. Among these methods, quantile mapping (QM) is widely used for its effectiveness in correcting biases across the entire distribution of climate variables(Ngai et al., 2017). QM operates by aligning the cumulative distribution functions (CDFs) of model simulations with those of observations, ensuring that both mean values and variability, including extremes, are accurately represented. This approach is particularly beneficial for variables like precipitation, where accurately capturing extreme events is crucial for hydrological modeling and climate impact studies.

Step 2: After the bias correction, the selected climate extreme indices were calculated by using Python. In climate research, selecting specific indices from the 27-core climate extreme indices defined by the Expert Team on Climate Change Detection and Indices is typically driven by the study's objectives, regional climatic characteristics and the relevance of the indices to the climate impacts under investigation(Donat et al., 2013). This study focused on three widely recognized indices Consecutive Dry Days, Consecutive Wet Days and heavy precipitation days due to their strong relevance in assessing precipitation variability and extremes. These indices directly represent key hydrometeorological conditions: drought duration, persistent wet periods and the frequency of heavy rainfall events, all of which have significant environmental and socio-economic implications(Sillmann et al., 2013). For instance, a study assessing the influence of climate change on multiple climate indices in Nepal utilized these indices to evaluate precipitation trends and model performance, highlighting their relevance in capturing key climatic features in the region. The extreme climate indices that were used are shown in Table 3

Table 4-2 The Climate Extreme Indices Used for This Study

	Climate Indices	**Indicator**	**Definitions**	**Units**
Duration	CDD	Consecutive Dry Days	Maximum number of consecutive days	Days
Duration	CWD	Consecutive Wet Days	Maximum number of consecutive days with rainfall ≥1mm	Days
Threshold	R10	Number of heavy precipitation days	Annual count of days when PRCP ≥ 10mm	Days

Step 3: The performance of selected GCMs was evaluated on the basics of performance statics: the CC, NMRSD, absolute NMRSD and AARD. Correlation Coefficient measures the strength and direction of the linear relationship between model predictions and observations. It indicates how well the model captures the variability in the observed data. NMRSD measures the performance of model by quantifying the difference between the predicted and observed values. The smaller the estimated NMSRD value, the better the model performance. ANMSRD gives the difference in the ratio between the observed and projected and the mean of observed values.

1. Correlation Coefficient (CC)

$$CC = \frac{\sum(X_i - \bar{X})(Y_i - \bar{Y})}{(T-1)S_X S_Y} \qquad \ldots\ldots\ldots\ldots (1)$$

This formula calculates how strongly the simulated values from the model align with the actual observed values. A higher value indicates a better correlation between the two datasets.

2. Normalized Root Mean Square (NMRSD)

$$NRMSD \frac{\sqrt{\frac{1}{T}\sum_{i=1}^{T}(x_i - y_i)^2}}{\bar{x}} = \qquad \ldots\ldots\ldots\ldots\ldots (2)$$

This measures how much the model's predictions deviate from the actual observations. A lower value means the model is performing well with minimal error.

3. Absolute Normalized Root Mean Square (ANMRSD)

$$ANRMSD = \left| \frac{\frac{1}{T}(\sum_{i=1}^{T}(y_i - x_i)}{\bar{x}} \right| \quad \ldots\ldots\ldots\ldots\ldots (3)$$

This is a variation of NRMSD, where the deviations between observed and simulated values are expressed as a ratio. Smaller values indicate better accuracy.

4. Average Absolute Relative Deviation (AARD)

$$AARD = \frac{1}{T}\sum_{i=1}^{T}\left|\frac{y_i - x_i}{x_i}\right| \quad \ldots\ldots\ldots\ldots\ldots (4)$$

This metric represents the average of relative errors in the model's predictions. Ideally, this value should be as close to zero as possible.

Where i=1, 2, 3, 4..., x_i represents observed values and y_i represents simulated values. T denotes the total number of time steps or observations.

Step 4: The entropy method was used to calculate the weight of each performance indicator. Entropy is used to determine the significance of each performance indicator. A higher entropy value means the indicator contributes less useful information to decision-making.

$$E_{nj} = -\frac{1}{\ln(T)}\sum_{a=1}^{T} q_{aj} \ln(q_{aj}) \quad \ldots\ldots\ldots\ldots\ldots (5)$$

$$Dd_j = 1 - E_{nj} \quad \ldots\ldots\ldots\ldots\ldots (6)$$

Where; q_{aj} - Normalized value from the payoff matrix, used in entropy calculation.

a- Represents the index for different climate models (RCMs).

j - Represents the index for different performance indicators.

E_{nj} -The calculated entropy value for an indicator.

Dd_j - Degree of diversification, which determines how informative an indicator is.

$$\gamma_j = \frac{Ddj}{\sum_{j=1}^{j} Ddj} \quad \ldots\ldots\ldots\ldots\ldots (7)$$

This formula calculates the normalized weight (γ_j) for each performance indicator. Dd_j is the degree of diversification for indicator j, determined using the entropy method. The denominator represents the sum of diversification values for all indicators, ensuring that the weights are proportionally distributed. The higher the weight (γ_j), the more influence that indicator has on evaluating the model's performance.

Step 5: Comprise programming was used to rank the performance of the GCMs. This programming is based on Euclidean theory. GCM having minimum value will be considered the most suitable and, ranking will be given on ascending value.

$$L_p(a) = [\sum_{j=1}^{J} w_j^p \left| f_j^* - f_{j(a)} \right|^p]^{\frac{1}{p}} \quad \ldots\ldots\ldots\ldots\ldots\ldots\ldots (8)$$

This equation is used to rank General Circulation Models (GCMs) based on their performance. $L_p(a)$ represents the ranking score for a given GCM (a). A lower value indicates a better-performing model. $f_j(a)$ is the normalized value of indicator j for model a. f_j^* is the ideal (best) value of indicator j. w_j is the weight assigned to indicator j, derived from the entropy method. p is a parameter that determines the ranking method (e.g., p=1 for linear ranking, p=2 for Euclidean distance).

5 RESULTS AND DISCUSSION

5.1 Evaluation of Observed Data and CMIP6 GCMs Climate Data

5.1.1 *Correlation coefficient*

The correlation coefficients for consecutive dry days, consecutive wet days and days with rainfall >10mm represent the relationship between observed data from the Department of Hydrology and Meteorology and the corresponding data derived from different General Circulation Models for Station 804, 808 and 1004. These correlations help assess how well each General Circulation Models aligns with observed climate patterns, offering insights into their reliability in capturing precipitation trends.

For Station 804: The results reveal interesting trends in model performance, with some models closely aligning with the observed data and others showing significant deviations.

Table 5-1 Correlation Coefficient among different indices at station 804

GCM	CDD	CWD	R10
ACESS-ESM-1.5	-0.02	-0.31	-0.16
EC-EARTH3-VEG	0.14	-0.05	-0.17
INM-CM4.8	0.03	0.05	-0.16
MIROC6	0.06	-0.02	0.07
MPI-ESM1.2-LR	-0.23	-0.29	-0.07
MRI- ESM2.0	-0.11	-0.02	-0.07
NESM3	0.01	0.05	-0.10

For CDD, most of the models show weak or very weak positive correlations with the observed data. This suggests that the models generally tend to predict a slightly higher number of consecutive dry days than what is actually observed at station 804. Among the models, MPI-ESM1.2-LR stands out with a strong negative correlation of -0.2263, indicating that this particular model significantly underestimates the number of consecutive dry days when compared to the observed data. Other models like ACESS-ESM-1.5 and MRI-ESM2.0 also show weak negative correlations -0.0182 and -0.1109 respectively implying that these models

slightly underestimate dry periods. On the other hand, models such as EC-EARTH3-VEG, INM-CM4.8 and MIROC6 show weak positive correlations ranging from 0.0085 to 0.1373, which suggests a minor overestimation of consecutive dry days compared to the observed data. Overall, the correlation coefficients for CDD across all models are relatively low, indicating that the models may not fully capture the observed patterns of consecutive dry days, with some overestimating and others underestimating the dry periods.

In the case of CWD, which tracks consecutive wet days, the correlation results indicate a trend of underestimating the number of wet days. The models that show the strongest negative correlations with observed data include ACESS-ESM-1.5 with a CC of -0.315 and MPI-ESM1.2-LR with a CC of -0.295, both of which significantly underestimate the number of consecutive wet days at station 804. This suggests that these models are predicting fewer wet days than what is actually observed. Other models, including EC-EARTH3-VEG with CC -0.055, MIROC6 with CC -0.02 and MRI-ESM2.0 with CC -0.021, show very weak negative correlations further indicating a slight underestimation of consecutive wet days. Only INM-CM4.8 with CC 0.053 and NESM3 with CC 0.048 show weak positive correlations, suggesting that these models may slightly overestimate the number of consecutive wet days, although the correlation is still very weak. The overall negative trend across most models in predicting CWD indicates a common issue of underestimating the frequency of wet spells, which could have implications for understanding precipitation patterns and hydrological processes in the region.

When it comes to R10, which refers to the number of extreme rainfall events, the correlation results reveal a general tendency for the models to underestimate the frequency of such events. All models, except for MIROC6, show weak to moderate negative correlations with observed R10 data. For example, ACESS-ESM-1.5 with CC -0.156, EC-EARTH3-VEG with CC -0.169 and INM-CM4.8 with CC -0.165 show moderate negative correlations, indicating that these models predict fewer extreme rainfall events than observed. MPI-ESM1.2-LR with CC -0.0678 and MRI-ESM2.0 with CC -0.071 show weaker negative correlations, but still indicate an under representation of extreme rainfall events. NESM3 with CC -0.097 also reflects this underestimation trend. MIROC6, however, stands as the exception with a very weak positive correlation having CC 0.068, suggesting that this model slightly overestimates extreme rainfall events compared to the observed data, although the correlation is still weak.

In summary, the analysis of the correlation coefficients reveals several important findings. Firstly, there is a consistent tendency among most of the GCMs to

underestimate CWD and R10, suggesting that these models struggle to accurately capture the frequency of wet spells and extreme rainfall events, both of which are critical for water resource management and flood prediction. Secondly, the models exhibit mixed results for CDD, with some models overestimating and others underestimating the number of consecutive dry days. The generally low correlation coefficients for CDD indicate that the models may not be well-suited to simulate this particular variable with high accuracy. Despite these weaknesses, model

s like INM-CM4.8 and MIROC6 show relatively better performance, particularly in simulating certain aspects of wet and dry periods.

For Station 808: The correlation coefficients for Station 808 illustrate the relationship between observed precipitation data and the projections from various General Circulation Models.

Table 5-2 Correlation Coefficient among different indices at station 808

GCM	CDD	CWD	R10
ACESS-ESM-1.5	-0.07	0.33	-0.17
EC-EARTH3-VEG	-0.24	0.06	-0.07
INM-CM4.8	-0.22	-0.07	0.11
MIROC6	-0.11	0.01	-0.21
MPI-ESM1.2-LR	0.38	-0.06	0.03
MRI- ESM2.0	0.04	0.01	-0.06
NESM3	-0.03	-0.29	-0.13

For CDD, the correlation values vary across models. MPI-ESM1.2-LR with CC 0.378 stands out with a strong positive correlation, suggesting that this model aligns well with the observed trend of consecutive dry days, making it potentially useful for drought prediction. MRI-ESM2.0 with a CC 0.038 has a weak positive correlation, indicating a slight alignment with observed data. However, most models, including EC-EARTH3-VEG having CC -0.239, INM-CM4.8 with -0.216 and MIROC6 has -0.109, display negative correlations, implying that they struggle to capture observed dry spell patterns accurately. ACCESS-ESM-1.5 has CC -0.071 and NESM3 has -0.025 also show weak negative correlations, suggesting minimal

agreement with observed trends. These findings highlight that while some models, like MPI-ESM1.2-LR, capture dry spells more effectively, others may underestimate or misrepresent the occurrence of prolonged dry periods.

For CWD, which measures the continuity of wet spells, the results vary significantly. ACCESS-ESM-1.5 has 0.326 shows the strongest positive correlation, suggesting that it effectively captures trends in consecutive wet days. EC-EARTH3-VEG has 0.060 and MRI-ESM2.0 has 0.009 have weak positive correlations, indicating a limited but positive relationship with observed wet spell trends. On the other hand, NESM3 with -0.292 has the strongest negative correlation, implying that it significantly underrepresents wet spells. INM-CM4.8 has -0.073 and MPI-ESM1.2-LR with -0.064 also show negative correlations, suggesting that these models may underestimate wet spell durations. MIROC6 with 0.008 has a near-zero correlation, indicating very little agreement with observed wet day patterns. The inconsistencies among models emphasize that while some align well with observed wet spells, others do not accurately reflect real-world precipitation patterns.

For R10, the models again exhibit varied performance. INM-CM4.8 having 0.107 and MPI-ESM1.2-LR with 0.031 have weak positive correlations, suggesting a slight agreement with observed extreme rainfall patterns. However, most models, including MIROC6 with -0.209, ACCESS-ESM-1.5 with -0.166, NESM3 with -0.126, EC-EARTH3-VEG with -0.073 and MRI-ESM2.0 with -0.062, show negative correlations, indicating that they generally underestimate the occurrence of heavy rainfall days. The negative correlation values suggest that these models do not capture the intensity or frequency of extreme rainfall events accurately, which could lead to limitations in their usefulness for predicting flood risks and heavy precipitation impacts.

Overall, the analysis of Station 408 reveals that different models perform differently depending on the climate index being analyzed. MPI-ESM1.2-LR exhibits the highest positive correlation for CDD, making it a potentially more reliable model for capturing dry spell trends. ACCESS-ESM-1.5 shows a strong positive correlation for CWD, suggesting that it aligns well with observed wet spell patterns. However, for R10, no model demonstrates a strong positive correlation, with most models failing to capture the occurrence of extreme rainfall days effectively. These inconsistencies indicate that while certain models can be useful for specific precipitation trends, none provide a universally reliable representation of all climate indices.

For Station 1004: Analyzing the correlation coefficient of station 1004 for CDD, CWD and R10.

Table 5-3 Correlation Coefficient among different indices at station 1004

GCM	CDD	CWD	R10
ACESS-ESM-1.5	-0.19	-0.36	-0.31
EC-EARTH3-VEG	0.04	0.08	-0.28
INM-CM4.8	0.27	0.01	0.02
MIROC6	-0.23	-0.10	0.30
MPI-ESM1.2-LR	-0.06	0.03	-0.16
MRI- ESM2.0	0.12	0.05	-0.36
NESM3	0.21	-0.02	-0.07

For CDD which represents the number of consecutive dry days, the correlation values vary across models. INM-CM4.8 with 0.269 and NESM3 with 0.207 show the highest positive correlations, indicating that these models tend to align more closely with observed trends of increasing dry spells. This suggests that these models might be more reliable in predicting prolonged dry periods. Conversely, MIROC6 having -0.230 and ACCESS-ESM-1.5 having -0.191 exhibit negative correlations, meaning these models deviate from observed data, potentially underestimating dry spells in the region. The mixed correlation results suggest that different models capture dry spell trends with varying degrees of accuracy, emphasizing the need for careful selection when applying GCM data for future projections.

For CWD, ACCESS-ESM-1.5 with CC -0.356 has the strongest negative correlation, indicating that it significantly underestimates observed wet spells. Similarly, MIROC6 having CC -0.098 and NESM3 with -0.025 also display weak negative correlations, suggesting discrepancies between these models and actual wet day observations. On the other hand, EC-EARTH3-VEG with 0.076, MRI-ESM2.0 with 0.049 and MPI-ESM1.2-LR having 0.0289 show weak positive correlations, implying that these models slightly align with observed wet spells but with limited accuracy. INM-CM4.8 with 0.01 has a near-zero correlation, suggesting little agreement with observed wet day trends. These variations highlight the challenges in accurately simulating wet spell durations, with most models showing weak correlations, either positive or negative.

For R10, which represents the number of days with rainfall exceeding 10mm, the results are also mixed. MIROC6 with 0.303 has the highest positive correlation, indicating that this model aligns relatively well with observed extreme rainfall events. This suggests that MIROC6 could be a more reliable model for projecting changes in heavy rainfall frequency. However, most other models, including MRI-ESM2.0 having -0.359, ACCESS-ESM-1.5 with -0.311 and EC-EARTH3-VEG with -0.277, show strong negative correlations, suggesting that these models tend to underestimate or misrepresent extreme rainfall events compared to observed data. INM-CM4.8 has 0.023 and MPI-ESM1.2-LR with -0.162 exhibit weaker correlations, indicating a limited match with observed extreme rainfall trends. The significant variation in correlation values suggests that while some models capture extreme rainfall patterns well, others fail to replicate observed trends accurately.

Overall, the correlation analysis reveals that no single model consistently aligns well with observed data across all three indices. MIROC6 shows a relatively strong correlation with extreme rainfall events, while INM-CM4.8 and NESM3 perform better in simulating consecutive dry days. However, models like ACCESS-ESM-1.5 and MRI-ESM2.0 exhibit weak or negative correlations across multiple indices, indicating a lower agreement with observed climate trends.

5.1.2 Normalized root mean square

The NRMSD is a measure of how well the GCMs replicate the observed data, with lower values indicating better agreement between the model outputs and observed data.

For Station 804: While analyzing CDD, most models exhibit relatively low NRMSD values, suggesting that they simulate the number of consecutive dry days with reasonable accuracy. The best-performing model in simulating CDD is MPI-ESM1.2-LR, with an NRMSD of 0.310, followed closely by EC-EARTH3-VEG and NESM3. However, INM-CM4.8 stands out with a much higher NRMSD of 0.669, indicating a poor fit to the observed CDD data.

Table 5-4 NRMSD among different indices at station 804

GCM	CDD	CWD	R10
ACESS-ESM-1.5	0.49	1.04	0.17
EC-EARTH3-VEG	0.33	1.14	0.17
INM-CM4.8	0.67	3.68	0.12
MIROC6	0.32	2.00	0.24
MPI-ESM1.2-LR	0.31	2.95	0.18
MRI- ESM2.0	0.26	2.48	0.17
NESM3	0.30	1.96	0.17

For CWD, the results show higher NRMSD values across most models, indicating that models struggle more with simulating consecutive wet days accurately. The worst-performing model in this regard is INM-CM4.8, with an NRMSD of 3.678, suggesting a significant discrepancy from the observed data. Models such as MPI-ESM1.2-LR having NRMSD 2.9526 and MIROC6 with 1.998 also show high NRMSD values, while ACESS-ESM-1.5 and EC-EARTH3-VEG perform somewhat better, with NRMSD values of 1.036 and 1.143, respectively. These results indicate that while some models are better at simulating CWD, all models tend to underestimate consecutive wet days and further refinement may be needed to improve accuracy.

For R10, the NRMSD values are relatively low, indicating that the models are generally better at simulating extreme rainfall events than consecutive wet days. The best-performing model for R10 is INM-CM4.8 as 0.1208, which shows a close fit to the observed data. It is followed by ACESS-ESM-1.5 with 0.174 and MPI-ESM1.2-LR with 0.179, both of which also show good agreement with the observed extreme rainfall events. However, MIROC6 has the highest NRMSD for R10 with 0.236, suggesting it slightly underperforms compared to the other models in simulating extreme rainfall events.

In conclusion, the analysis reveals that while most models perform reasonably well for CDD and R10, they tend to underperform for CWD, with some models showing significant deviations from the observed data. INM-CM4.8 stands out as the best model for Extreme Rainfall Events, while MPI-ESM1.2-LR is the best for consecutive dry days. However, all models struggle with accurately simulating consecutive wet days, highlighting a key area where GCMs could be improved.

These findings suggest that while GCMs can provide useful projections for certain climate variables, they still have limitations in replicating certain climate patterns, especially in regions like station 804.

For Station 808: Starting with consecutive dry days, the NRMSD values are relatively moderate across all models. The best-performing model for CDD is MIROC6 with an NRMSD of 0.2811, showing good agreement with the observed data. Other models such as EC-EARTH3-VEG with NRMSD as 0.322 and MPI-ESM1.2-LR with 0.422 also exhibit reasonable performance, though they show slightly higher deviations from the observed CDD values. NESM3 and ACESS-ESM-1.5 show higher NRMSD values 0.572 and 0.504, respectively, indicating that these models have a bit more difficulty in accurately replicating consecutive dry days. Overall, CDD is relatively well-represented by the models, with MIROC6 performing the best in this regard.

Table 5-5 NRMSD among different indices at station 808

GCM	CDD	CWD	R10
ACESS-ESM-1.5	0.50	1.76	0.34
EC-EARTH3-VEG	0.32	0.69	0.22
INM-CM4.8	0.67	2.31	0.29
MIROC6	0.28	1.72	0.25
MPI-ESM1.2-LR	0.42	1.47	0.22
MRI- ESM2.0	0.53	2.42	0.25
NESM3	0.57	1.78	0.22

When it comes to Consecutive Wet Days, there is a wider variation in model performance. EC-EARTH3-VEG stands out with an NRMSD of 0.691, indicating the best fit to the observed CWD data. This suggests that it performs relatively well in simulating the frequency of wet periods. However, other models such as MIROC6 with 1.724 and ACESS-ESM-1.5 with 1.759 show higher NRMSD values, indicating a higher degree of deviation from the observed consecutive wet days. INM-CM4.8 having NRMSD 2.306, MPI-ESM1.2-LR having 1.467 and MRI-ESM2.0 as 2.422 have even higher NRMSD values, showing that they significantly underestimate or fail to replicate the frequency of consecutive wet days. The results for CWD suggest that this variable is more challenging for most models, with EC-EARTH3-VEG performing relatively better, but still leaving room for improvement.

For R10, the models generally perform reasonably well, although there is some variation in their accuracy. The best-performing model for R10 is ACESS-ESM-1.5 with NRMSD as 0.337, followed closely by INM-CM4.8 with 0.297, which also show good agreement with the observed extreme rainfall events. EC-EARTH3-VEG has 0.216 also shows relatively good performance, while MIROC6 with 0.250 exhibits slightly weaker performance, although still within a reasonable range. NESM3 as 0.218 and MPI-ESM1.2-LR with 0.217 show similar NRMSD values, indicating their reasonably good ability to simulate extreme rainfall events, with some minor deviations. The worst-performing model for R10 is MRI-ESM2.0 with 0.248, though it still provides a relatively good fit.

In conclusion, the analysis reveals that for CDD, most models perform well, with MIROC6 showing the best fit. For CWD, EC-EARTH3-VEG performs the best, though it still shows some deviation from observed data. Models struggle more with simulating CWD, with INM-CM4.8, MPI-ESM1.2-LR and MRI-ESM2.0 showing significant discrepancies. For R10, most models show reasonable performance, with ACESS-ESM-1.5 performing the best, followed closely by INM-CM4.8 and EC-EARTH3-VEG. Overall, R10 is the variable most accurately simulated by the models, while CWD presents the most significant challenge across the board.

For Station 1004: The analysis of Normalized Root Mean Square Deviation between the observed data and outputs from various Global Climate Models reveals differing levels of accuracy in simulating key climate variables, namely Consecutive Dry Days, Consecutive Wet Days and Number of Heavy Precipitation Days.

Table 5-6 NRMSD among different indices at station 1004

GCM	CDD	CWD	R10
ACESS-ESM-1.5	0.61	1.57	0.30
EC-EARTH3-VEG	0.41	0.97	0.15
INM-CM4.8	0.26	0.01	0.18
MIROC6	0.39	1.09	0.23
MPI-ESM1.2-LR	0.42	0.52	0.16
MRI- ESM2.0	0.40	0.97	0.20
NESM3	0.43	0.97	0.16

For CDD, INM-CM4.8 performs the best, with the lowest NRMSD of 0.262, suggesting it provides the most accurate simulation of consecutive dry days among the models. EC-EARTH3-VEG and MIROC6 also show relatively low NRMSD values, indicating that these models are reasonably good at simulating dry periods, but ACESS-ESM-1.5 has the highest NRMSD with 0.611, showing that it struggles more in simulating CDD compared to other models.

For CWD, INM-CM4.8 excels with an exceptionally low NRMSD of 0.01, suggesting it is far superior in replicating consecutive wet days. In contrast, ACESS-ESM-1.5 as 1.57 and MIROC6 with 1.09 show much higher NRMSD values, indicating a weaker performance in simulating consecutive wet days. MPI-ESM1.2-LR and NESM3 perform better than the latter models but still have higher NRMSD values than INM-CM4.8, highlighting that simulating wet periods is more challenging for most GCMs.

When analyzing R10, EC-EARTH3-VEG emerges as the best-performing model with an NRMSD of 0.15 closely followed by INM-CM4.8 with 0.18 and MIROC6 with 0.23. These models show a good fit to the observed extreme rainfall events. ACESS-ESM-1.5 with 0.30 has the highest NRMSD for R10, indicating it is less accurate in simulating extreme rainfall compared to other models, though it still provides a reasonable fit. Overall, the results show that INM-CM4.8 is the best model for simulating CWD, while EC-EARTH3-VEG performs best for R10. ACESS-ESM-1.5 appears to be the weakest in simulating CDD and CWD, while performing reasonably well for R10. These findings suggest that while some models perform well in simulating certain variables, there are still areas, particularly in CWD, where further improvements are needed to better replicate observed climate patterns at Station 1004.

In conclusion, the analysis of Stations 804, 808 and 1004 shows that INM-CM4.8 consistently performs the best in simulating Consecutive Dry Days and Consecutive Wet Days across all stations, with particularly strong results for CWD. EC-EARTH3-VEG performs well for Extreme Rainfall Events, particularly at Stations 808 and 1004. While MIROC6 and NESM3 show good performance for R10, ACESS-ESM-1.5 tends to underperform, especially in simulating CWD. Overall, the models generally perform well in simulating CDD and R10, but simulating CWD remains a challenge, highlighting the need for further improvements.

5.1.3 Absolute nnormalized root mean square

The Absolute Normalized Root Mean Square Deviation (ANMRSD) values between the observed data and outputs from various Global Climate Models for Station 804, 808 and 1004 provide an indication of the models' performance in simulating climate variables such as Consecutive Dry Days, Consecutive Wet Days and Extreme Rainfall Events. Lower ANMRSD values indicate better model performance and closer alignment with the observed data.

For Station 804: The analysis of the Absolute Normalized Root Mean Square Deviation (ANMRSD) values for Station 404 provides valuable insights into how different Global Climate Models simulate key climate variables: Consecutive Dry Days, Consecutive Wet Days and Extreme Rainfall Events.

Table 5-7 ANRMSD among different indices at station 804

GCM	CDD	CWD	R10
ACESS-ESM-1.5	0.04	0.61	0.00
EC-EARTH3-VEG	0.12	0.85	0.12
INM-CM4.8	0.58	3.59	0.12
MIROC6	0.14	1.71	0.11
MPI-ESM1.2-LR	0.19	2.73	0.12
MRI- ESM2.0	0.10	2.27	0.12
NESM3	0.07	1.72	0.11

ACESS-ESM-1.5 stands out as the best-performing model overall, with the lowest ANMRSD values for both CDD with 0.034 and R10 with 0.0003, suggesting that it is highly effective in simulating dry periods and extreme rainfall events at Station 804. The model's performance in simulating CDD is particularly strong, as it closely matches the observed data. This indicates that ACESS-ESM-1.5 is highly accurate in replicating dry spells, which is crucial for understanding drought conditions and managing water resources. In terms of R10, ACESS-ESM-1.5 also provides an excellent fit, with a nearly perfect match to the observed extreme rainfall events. The very low ANMRSD value for R10 indicates that ACESS-ESM-1.5 effectively captures extreme precipitation events, which is essential for understanding flood risks and extreme weather patterns. However, ACESS-ESM-1.5 has a relatively higher ANMRSD for CWD having 0.60, suggesting that while it

performs well in simulating dry periods and extreme rainfall, it faces challenges in replicating wet periods accurately. This indicates that ACESS-ESM-1.5 may not be as well-suited for modeling extended wet spells, which could have implications for flood modeling and water resource management during wetter seasons. MIROC6 performs well, particularly for R10, with an ANMRSD value of 0.16, showing a good match to the observed extreme rainfall data. However, it lags behind ACESS-ESM-1.5 in both CDD and CWD simulations, with CDD showing an ANMRSD of 0.145 and CWD of 1.71. Although MIROC6 does not perform as well as ACESS-ESM-1.5 for dry days and wet days, it still provides valuable insights into the patterns of extreme rainfall, which could be useful for certain flood-related studies or understanding precipitation extremes. The model's relatively higher ANMRSD for CWD suggests that MIROC6 struggles more with simulating consecutive wet days compared to ACESS-ESM-1.5. This could be due to its inability to capture the full dynamics of wet spells, making it less reliable for studies focused on rainfall distribution during extended wet periods. INM-CM4.8 exhibits notable weaknesses in simulating both CDD and CWD, particularly for CWD where it has the highest ANMRSD value of 3.59. This indicates that INM-CM4.8 deviates significantly from the observed data when modeling consecutive wet days, suggesting it struggles with wet period simulation. While INM-CM4.8 is able to simulate R10 reasonably well, with an ANMRSD of 0.12, its overall performance in replicating the patterns of consecutive dry and wet days at Station 804 is poor. This model's high ANMRSD for CWD suggests that it may not be suitable for studies focused on the dynamics of wet periods and it may need further calibration or improvements to capture these phenomena more accurately. MPI-ESM1.2-LR and MRI-ESM2.0 show moderate performance across the three variables. MPI-ESM1.2-LR has ANMRSD values of 0.187 for CDD, 2.73 for CWD and 0.12 for R10, while MRI-ESM2.0 shows ANMRSD values of 0.1, 2.28 and 0.12, respectively. While both models show decent fits for CDD and R10, they also show relatively higher deviations for CWD. MPI-ESM1.2-LR and MRI-ESM2.0 perform better than INM-CM4.8 in simulating CWD, but their performance still lags behind ACESS-ESM-1.5 and MIROC6. The higher ANMRSD values for CWD suggest that these models, while reasonably good at simulating dry days and extreme rainfall, face significant challenges in replicating the observed wet periods at Station 404. NESM3 performs better than INM-CM4.8 for CWD, with an ANMRSD of 1.72, but it is still not as accurate as ACESS-ESM-1.5 or MIROC6. For CDD, NESM3 with 0.07 performs better than several other models, but still shows a deviation from the observed data. For R10, NESM3 with 0.12 is relatively competitive, though ACESS-ESM-1.5 remains the best model in this regard.

For Station 808: Among the evaluated models, ACESS-ESM-1.5 demonstrates a moderate deviation for CDD with ANRMSD 0.24 and a relatively high deviation for CWD with 1.43, but it performs exceptionally well for R10 with 0.01, suggesting its accuracy in simulating extreme rainfall events.

Table 5-8 ANRMSD among different indices at station 808

GCM	CDD	CWD	R10
ACESS-ESM-1.5	0.24	1.43	0.01
EC-EARTH3-VEG	0.03	0.56	0.15
INM-CM4.8	0.38	2.10	0.17
MIROC6	0.10	1.39	0.15
MPI-ESM1.2-LR	0.15	1.27	0.16
MRI- ESM2.0	0.33	2.15	0.16
NESM3	0.37	1.57	0.15

On the other hand, EC-EARTH3-VEG performs exceptionally well for CDD with value of NRMSD as 0.03, showing minimal deviation from observed values and also demonstrates the lowest ANMRSD for CWD with 0.56, indicating that it is the most reliable model for simulating both dry and wet periods. However, its R10 value is 0.15 is higher than that of ACESS-ESM-1.5, indicating that it is slightly less precise in capturing extreme rainfall occurrences. INM-CM4.8 exhibits higher deviations across all three variables, with ANMRSD values of 0.3784 for CDD, 2.10 for CWD and 0.17 for R10, suggesting that this model struggles with simulating consecutive wet days and may not be the best option for capturing extreme precipitation events at this station. MIROC6, on the other hand, has a low ANMRSD for CDD with 0.10, indicating a good representation of dry days, while its values for CWD with 1.39 and R10 with 0.15 indicate a moderate performance for wet spells and extreme rainfall events.

Similarly, MPI-ESM1.2-LR performs moderately across all variables, with ANRMSD values of 0.1481 for CDD, 1.2692 for CWD and 0.1550 for R10. It does not significantly outperform other models in any specific category but remains fairly balanced. MRI-ESM2.0 exhibits a slightly higher ANMRSD for CDD with 0.36 and CWD with 2.19, indicating notable deviations in these variables, while its R10

value is 0.16 remains moderate. Similarly, NESM3 follows a comparable pattern with ANMRSD values of 0.39 for CDD, 1.57 for CWD and 0.15 for R10, demonstrating a somewhat higher deviation in dry day simulations but a relatively better performance for extreme rainfall events.

Overall, the analysis highlights that EC-EARTH3-VEG is the most reliable model for simulating both dry and wet periods due to its low ANMRSD for CDD and CWD, while ACESS-ESM-1.5 is the best model for extreme rainfall events due to its minimal ANMRSD for R10. Conversely, models such as INM-CM4.8, MRI-ESM2.0 and NESM3 show considerable deviations, particularly in their ability to simulate consecutive wet days, indicating that further improvements may be needed in their precipitation modeling capabilities. These findings emphasize the need for careful model selection based on the specific hydrological and meteorological parameters of interest.

For Station 1004: Among the models, ACESS-ESM-1.5 exhibits a moderate ANMRSD for CDD with 0.26 and CWD with 0.92, but it stands out for its remarkable accuracy in extreme rainfall simulations, with an ANMRSD of just 0.002 for R10.

Table 5-9 ANRMSD among different indices at station 1004

GCM	CDD	CWD	R10
ACESS-ESM-1.5	0.26	0.92	0.00
EC-EARTH3-VEG	0.13	0.95	0.05
INM-CM4.8	0.08	0.25	0.04
MIROC6	0.15	0.55	0.04
MPI-ESM1.2-LR	0.06	0.06	0.05
MRI- ESM2.0	0.08	0.52	0.05
NESM3	0.05	0.58	0.05

This suggests that ACESS-ESM-1.5 is highly reliable for extreme precipitation events at this station, though it shows some deviations in dry and wet spell simulations. EC-EARTH3-VEG performs well in simulating CDD with 0.13 but has a slightly higher ANMRSD for CWD with 0.95, indicating that it captures dry days better than wet spells. Its R10 value with 0.05 is relatively higher compared to ACESS-ESM-1.5, suggesting slightly less accuracy in simulating extreme rainfall. INM-CM4.8, on the other hand, exhibits the lowest ANMRSD for CDD is 0.08 and a

relatively low deviation for CWD is 0.25, making it one of the best-performing models in simulating both dry and wet periods. Its R10 value with 0.04 is also low, showing that INM-CM4.8 is well-suited for capturing overall precipitation patterns at this station. MIROC6 demonstrates moderate performance across all parameters, with ANRMSD values of 0.15 for CDD, 0.55 for CWD and 0.04 for R10, suggesting it is fairly balanced but does not outperform INM-CM4.8 or ACESS-ESM-1.5 in any specific category. MPI-ESM1.2-LR stands out with the lowest ANRMSD for CWD with 0.06 and a low CDD value with 0.06, indicating that this model performs exceptionally well in capturing both dry and wet periods. However, its R10 value is 0.05 is slightly higher than that of ACESS-ESM-1.5 and INM-CM4.8, meaning it is slightly less accurate for extreme precipitation. MRI-ESM2.0 and NESM3 follow a similar trend, with relatively low ANRMSD values for CDD is 0.06 and 0.05, respectively and moderate CWD deviations with 0.52 and 0.58, respectively. Their R10 values both around 0.0494–0.0475 indicate reasonable performance for extreme rainfall events, but they do not outperform ACESS-ESM-1.5 in this category.

Overall, INM-CM4.8 and MPI-ESM1.2-LR emerge as the best models for simulating dry and wet spells, with ACESS-ESM-1.5 excelling in capturing extreme rainfall events. The models generally exhibit better performance in simulating CDD and CWD compared to R10, with ACESS-ESM-1.5 significantly outperforming others in extreme rainfall accuracy. This suggests that selecting the appropriate GCM depends on the specific hydrological parameter of interest, with INM-CM4.8 and MPI-ESM1.2-LR being preferable for seasonal precipitation trends, while ACESS-ESM-1.5 is best suited for extreme event studies.

5.1.4 Average absolute relative deviation

The Average Absolute Relative Deviation provides insight into how well different Global Climate Models align with observed data from the Department of Hydrology and Meteorology in terms of Consecutive Dry Days, Consecutive Wet Days and Extreme Rainfall Events. A lower AARD value indicates better model accuracy in capturing observed climatic patterns.

For Station 804: Among the analyzed models, ACESS-ESM-1.5 shows a moderate deviation for CDD is 0.45 and CWD is 0.43 but performs relatively well for R10 with 0.13, suggesting it provides a reasonable estimate of extreme rainfall events at this station. EC-EARTH3-VEG, on the other hand, exhibits a lower AARD for CDD having value of 0.33 and the lowest R10 deviation with 0.11, making it the most reliable model for capturing dry days and extreme rainfall.

Table 5-10 AARD among different indices at station 804

GCM	CDD	CWD	R10
ACESS-ESM-1.5	0.45	0.43	0.13
EC-EARTH3-VEG	0.33	0.69	0.11
INM-CM4.8	0.82	2.77	0.15
MIROC6	0.34	1.33	0.16
MPI-ESM1.2-LR	0.34	2.11	0.13
MRI- ESM2.0	0.29	1.76	0.12
NESM3	0.30	1.33	0.13

However, its CWD value as 0.69 is slightly higher than that of ACESS-ESM-1.5, indicating a moderate deviation in simulating wet spells. INM-CM4.8 demonstrates the highest AARD for CDD with 0.82 and CWD with 2.77, which suggests significant deviations from observed values, making it the least accurate model in simulating dry and wet spells. Its R10 value 0.15 is also among the highest, further indicating that this model may not be the best fit for precipitation event simulations at this station. MIROC6 performs moderately, with AARD values of 0.34 for CDD, 1.33 for CWD and 0.16 for R10, suggesting it captures dry days well but exhibits notable deviations in consecutive wet days and extreme rainfall. MPI-ESM1.2-LR follows a similar pattern, with AARD values of 0.34 for CDD, 2.11 for CWD and 0.13 for R10, indicating significant deviation in wet spell simulations but reasonable accuracy in extreme rainfall events. MRI-ESM2.0 and NESM3 show comparable results, with relatively low deviations for CDD is 0.29 and 0.30, respectively and moderate CWD deviations 1.76 and 1.33, respectively. Their R10 values 0.12 and 0.13, respectively suggest they are reasonably accurate in capturing extreme rainfall.

In summary, EC-EARTH3-VEG emerges as the most reliable model for dry days and extreme rainfall, with ACESS-ESM-1.5 also performing well for extreme rainfall. INM-CM4.8 exhibits the highest deviations, particularly for CDD and CWD, making it the least suitable model for this station. MRI-ESM2.0 and NESM3 provide a balanced performance, while MIROC6 and MPI-ESM1.2-LR show moderate deviations in wet spell simulations. This analysis suggests that model selection should depend on the specific hydrological variable of interest, with EC-EARTH3-VEG being preferable for dry days and extreme events, while models like MRI-

ESM2.0 and NESM3 may offer a more balanced representation of overall precipitation trends.

For Station 808: The table below presents AARD values between the values of different GCMs and the observed values from the Department of Hydrology and Meteorology of Nepal.

Table 5-11 AARD among different indices at station 808

GCM	CDD	CWD	R10
ACESS-ESM-1.5	0.34	2.38	0.24
EC-EARTH3-VEG	0.25	0.79	0.22
INM-CM4.8	0.38	2.93	0.28
MIROC6	0.25	1.95	0.24
MPI-ESM1.2-LR	0.32	1.77	0.21
MRI- ESM2.0	0.38	2.99	0.24
NESM3	0.43	2.19	0.21

Among the GCMs, EC-EARTH3-VEG demonstrates the lowest AARD for CDD is 0.25 and CWD is 0.79, indicating that this model performs best in simulating dry and wet spells. It also provides a reasonably low deviation for R10 with value of 0.22, making it one of the more reliable models overall for this station. MIROC6 follows closely, with an AARD of 0.25 for CDD, a slightly higher 1.95 for CWD and 0.24 for R10, suggesting that while it effectively captures dry days, its performance in simulating wet spells is slightly less accurate than EC-EARTH3-VEG. On the other hand, INM-CM4.8 and MRI-ESM2.0 exhibit the highest deviations for CDD 0.38 and 0.38, respectively and CWD 2.93 and 2.99, respectively, suggesting that these models struggle to replicate observed dry and wet spell trends. Their R10 values 0.29 and 0.24, respectively indicate that they are less reliable for predicting extreme rainfall events. Similarly, NESM3 shows high deviation in CDD with 0.43 and CWD with 2.19 but has a relatively lower R10 deviation of 0.20, making it less accurate for consecutive dry and wet days but moderately effective for extreme rainfall. ACESS-ESM-1.5 and MPI-ESM1.2-LR fall into the mid-range category. ACESS-ESM-1.5 has an AARD of 0.3353 for CDD, indicating moderate accuracy in capturing dry spells. However, its CWD deviation (2.3786) is relatively high, meaning it struggles with wet spell representation. Its R10 value 0.24 suggests moderate accuracy for extreme events. MPI-ESM1.2-LR, on the other hand,

exhibits AARD values of 0.32 for CDD, 1.77 for CWD and 0.20 for R10, making it a relatively balanced model that performs moderately well in all categories.

In summary, EC-EARTH3-VEG emerges as the most reliable model for Station 408, particularly in simulating dry and wet spells, while MIROC6 also performs well in capturing dry days. INM-CM4.8 and MRI-ESM2.0 exhibit the highest deviations, making them the least suitable models for this station. NESM3 struggles with dry and wet spells but provides a reasonable estimate for extreme rainfall. MPI-ESM1.2-LR and ACESS-ESM-1.5 offer a balanced performance, with moderate deviations across all categories. Therefore, for applications requiring accurate simulation of dry and wet spells, EC-EARTH3-VEG is the preferred model, whereas MIROC6 and MPI-ESM1.2-LR may be considered for general rainfall trend analysis.

For Station 1004: The Average Absolute Relative Deviation (AARD) values for Station 1004 provide a comparative assessment of how well different Global Climate Models simulate observed data from the Department of Hydrology and Meteorology (DHM) in terms of Consecutive Dry Days, Consecutive Wet Days and Extreme Rainfall Events. Lower AARD values indicate better alignment with observed data, while higher values suggest greater deviation.

Table 5-12 AARD among different indices at station 1004

GCM	CDD	CWD	R10
ACESS-ESM-1.5	0.25	0.41	0.15
EC-EARTH3-VEG	0.26	0.54	0.12
INM-CM4.8	0.17	0.26	0.14
MIROC6	0.25	0.43	0.17
MPI-ESM1.2-LR	0.27	0.25	0.13
MRI- ESM2.0	0.23	0.41	0.15
NESM3	0.28	0.42	0.13

Among the models, INM-CM4.8 demonstrates the lowest deviation for CDD with value of 0.18 and CWD with 0.26, indicating a strong capability to simulate dry and wet spells with relatively high accuracy. Its R10 deviation is 0.14 which is also moderately low, making it one of the more reliable models overall for this station. Similarly, MPI-ESM1.2-LR shows a low AARD of 0.2532 for CWD, suggesting it

performs well in capturing wet spells. However, its CDD with 0.27 and R10 having 0.13 deviations indicate slightly higher error margins compared to INM-CM4.8. EC-EARTH3-VEG also performs well, particularly in extreme rainfall simulations, with an AARD of 0.12 for R10, the lowest among all models. However, its CDD deviation 0.26 is slightly higher and its CWD deviation is 0.54 suggests moderate reliability in simulating wet spells. MIROC6 and ACESS-ESM-1.5 show comparable performances, with CDD deviations of 0.25 and 0.25, respectively and CWD deviations of 0.43 and 0.41, respectively. Their R10 deviations is 0.17 for MIROC6 and 0.15 for ACESS-ESM-1.5 indicate moderate performance in extreme rainfall simulations. On the other hand, MRI-ESM2.0 and NESM3 exhibit slightly higher deviations across multiple parameters. MRI-ESM2.0 shows moderate performance in dry and wet spells, with AARD values of 0.23 for CDD and 0.41 for CWD, but its R10 deviation is 0.15 is comparable to some of the better-performing models. NESM3, however, has the highest CDD deviation as 0.28 and CWD deviation is 0.42, suggesting that it is less reliable for simulating dry and wet spell occurrences. Its R10 deviation is 0.13 which is moderate, making it slightly more suitable for extreme rainfall estimates than for consecutive dry and wet day predictions.

In summary, INM-CM4.8 emerges as the most reliable model for Station 1004, particularly in simulating dry and wet spells, while EC-EARTH3-VEG performs best in capturing extreme rainfall events. MPI-ESM1.2-LR also shows strong performance for wet spells, while MIROC6 and ACESS-ESM-1.5 demonstrate balanced performance across all parameters. MRI-ESM2.0 and NESM3 exhibit higher deviations, making them less suitable for accurately simulating dry and wet days. Thus, for applications requiring precise climate modeling, INM-CM4.8 and EC-EARTH3-VEG are the preferred choices, while MPI-ESM1.2-LR, MIROC6 and ACESS-ESM-1.5 may be considered for general trend analyses.

5.2 Variation of Performance Indicators for Particular Indices of Different Stations

5.2.1 Correlation coefficient

The figure 3 shows the variation of Consecutive Dry Days, the correlation coefficients between DHM observations and GCM outputs show mixed trends across stations 804, 808 and 1004, with models performing inconsistently. At Station 808, MPI-ESM1.2-LR with CC 0.38 exhibits a strong positive correlation,

indicating that it aligns well with observed dry spell trends, making it a potentially reliable model for drought predictions. However, most other models at this station, including EC-EARTH3-VEG having CC -0.24, INM-CM4.8 with -0.22 and MIROC6 with -0.11, show negative correlations, suggesting they underestimate dry spell duration. At Station 1004, INM-CM4.8 has CC 0.27 and NESM3 has 0.21 display moderate positive correlations, indicating better alignment with observed data, whereas MIROC6 has -0.23 and ACCESS-ESM-1.5 has -0.19 show negative correlations, suggesting underestimation of consecutive dry days. At Station 804, most models exhibit weak correlations, with MPI-ESM1.2-LR having -0.23 and MRI-ESM2.0 having -0.12 having negative values, indicating poor model performance in simulating dry spells. Overall, no single GCM consistently aligns with observed CDD trends across all stations, though MPI-ESM1.2-LR performs well at Station 808 and INM-CM4.8 and NESM3 show better agreement at Station 1004.

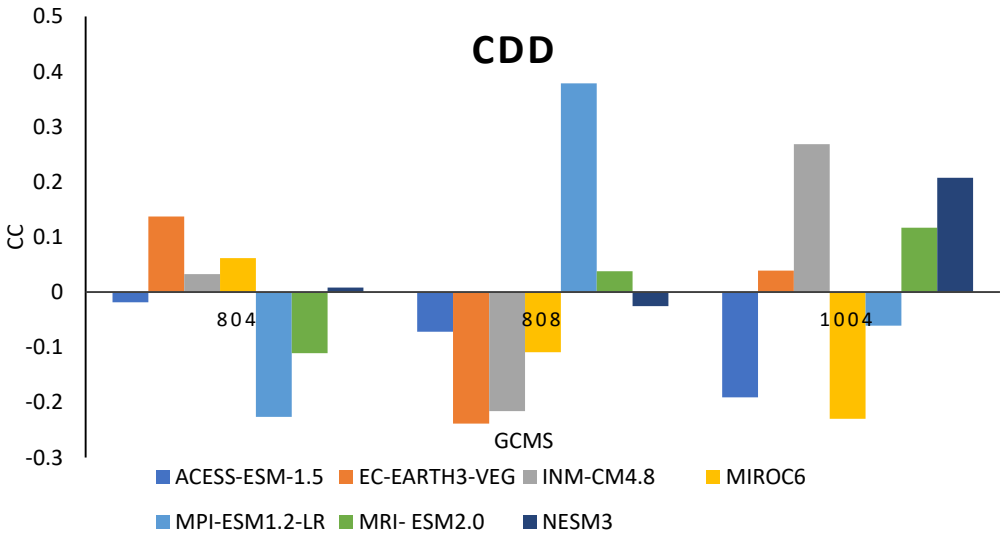

Figure 5-1 Variation of CC for the CDD index across different stations.

The correlation coefficients for Consecutive Wet Days across different General Circulation Models at stations 804, 808 and 1004 in figure 4 show a range of behaviors in terms of wet period predictions. For Consecutive Wet Days, the correlation coefficients indicate that most GCMs underestimate wet spell durations, particularly at Station 804, where models like ACCESS-ESM-1.5 with CC -0.31 and MPI-ESM1.2-LR with -0.295 show strong negative correlations, suggesting a significant underrepresentation of consecutive wet days. Similar trends are seen at Station 1004, where ACCESS-ESM-1.5 having CC -0.35 also

exhibits a strong negative correlation, reinforcing its poor ability to simulate wet periods accurately. However, at Station 808, ACCESS-ESM-1.5 with CC 0.33 stands out with a strong positive correlation, indicating better performance in capturing wet spell trends. Other models, such as EC-EARTH3-VEG, MIROC6 and MRI-ESM2.0, display weak positive correlations at some stations but remain inconsistent overall, while NESM3 with -0.29 at Station 808 has a strong negative correlation, suggesting poor performance in simulating consecutive wet days. Overall, most models struggle to represent wet spells accurately, with general underestimation trends, except for ACCESS-ESM1.5 at Station 808, which performs relatively well.

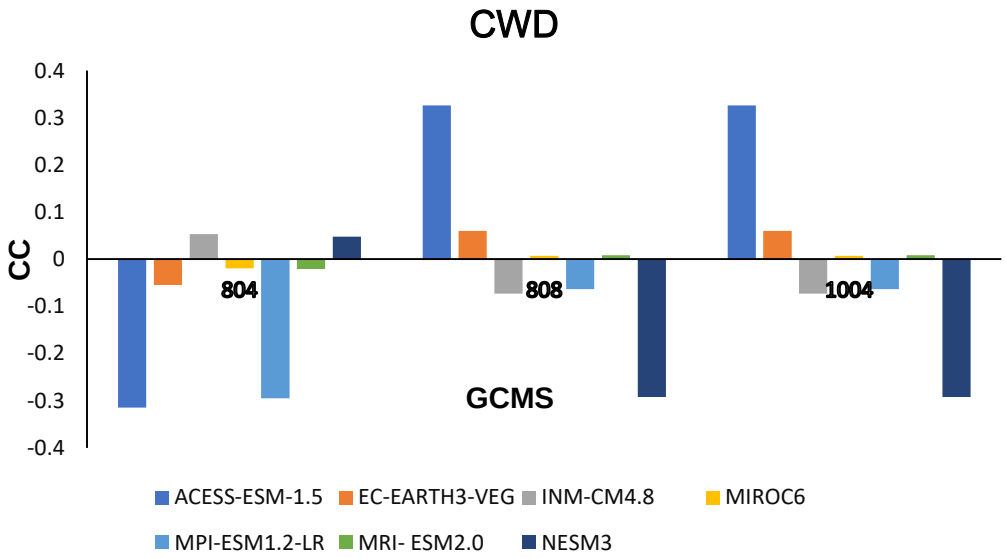

Figure 5-2 Variation of CC for the CWD index across different stations.

The correlation coefficients between DHM observations and GCM outputs for R10 across stations 804, 808 and 1004 reveal a general tendency for models to underestimate extreme rainfall events. Most CCs are negative, indicating poor alignment between GCM projections and observed data, particularly at Station 1004, where MRI-ESM2.0 with -0.36, ACESS-ESM-1.5 with -0.31 and EC-EARTH3-VEG with -0.28 show strong negative correlations, suggesting these models significantly underpredict heavy rainfall days. However, MIROC6 with 0.30 at Station 1004 and INM-CM4.8 with 0.11 at Station 808 show weak positive correlations, indicating slightly better performance in simulating extreme rainfall patterns at these locations. Other models, such as MPI-ESM1.2-LR and NESM3, consistently exhibit weak negative correlations across all stations, implying systematic underrepresentation of heavy rainfall trends. Overall, the results suggest that most GCMs struggle to replicate extreme rainfall events accurately

compared to DHM data, with a general tendency toward underestimation, while MIROC6 and INM-CM4.8 perform relatively better at specific stations but not consistently across all locations.

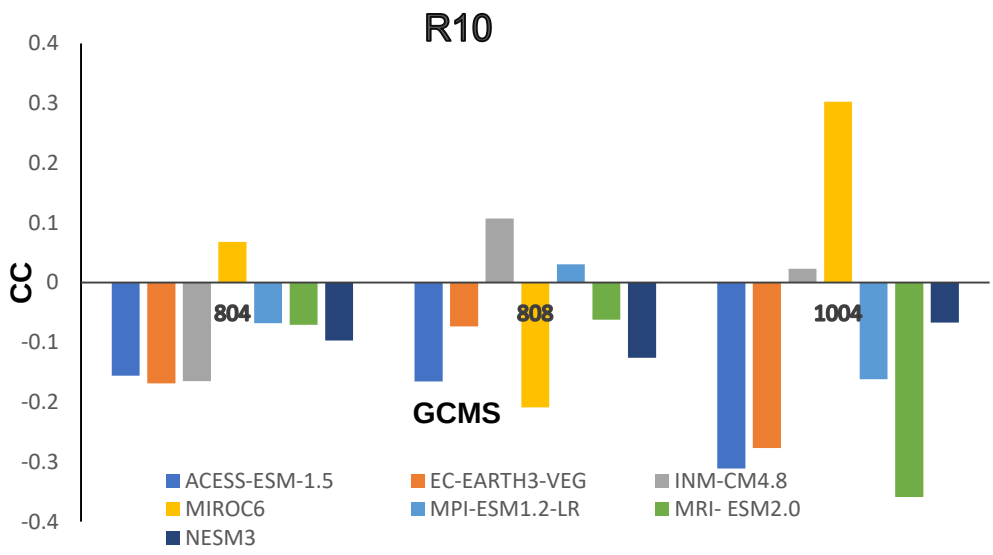

Figure 5-3 Variation of CC for the R10 index across different stations.

5.2.2 Normalized root mean square

The Normalized Root mean Square Deviation values for Consecutive Dry Days across different GCMs indicate variations in model accuracy when compared to DHM observations. At Station 804, the INM-CM4.8 model with NRMSD 0.67 exhibits the highest NRMSD, suggesting a relatively larger deviation from observed data, while MRI-ESM2.0 with 0.27 has the lowest, indicating better performance. A similar trend is observed at Station 808, where INM-CM4.8 with value of 0.67 and NESM3 with 0.57 show higher deviations, whereas MRI-ESM2.0 having 0.53 and ACCESS-ESM-1.5 with 0.50 exhibit moderate alignment. At Station 1004, ACCESS-ESM-1.5 0.61 has the highest NRMSD, while INM-CM4.8 with 0.26 shows the least deviation, suggesting that its dry spell estimates align better with observed values at this location. MPI-ESM1.2-LR and NESM3 exhibit moderate deviations at all three stations. Overall, most models display significant deviations in simulating CDD, with INM-CM4.8 performing better at Station 1004 but showing large errors at other stations, whereas MRI-ESM2.0 has the smallest deviations at Station 804.

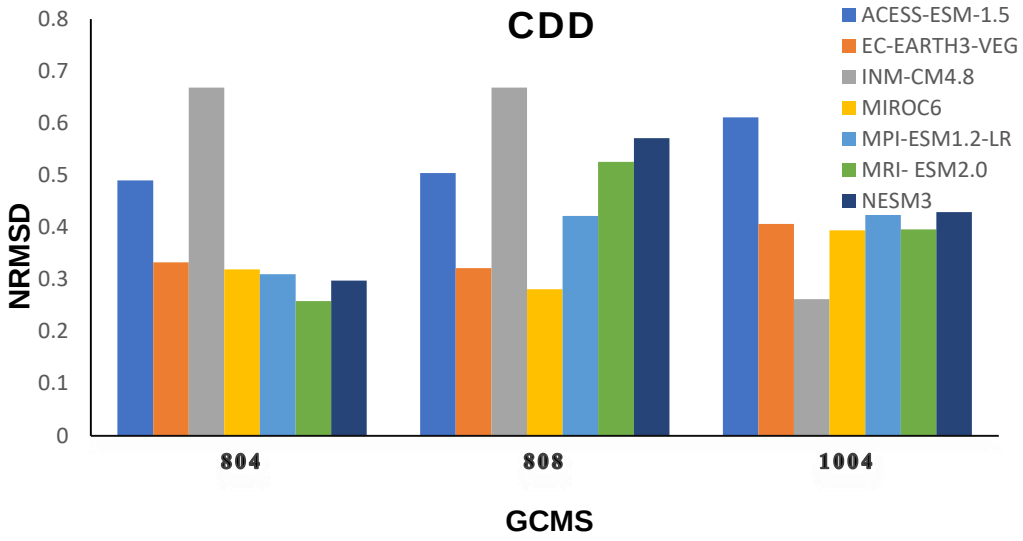

Figure 5-4 Variation of NRMSD for the CDD index across different stations.

The Normalized Root Mean Square Deviation values for Consecutive Wet Days across different GCMs reveal significant variations in model performance compared to DHM observations. At Station 804, INM-CM4.8 having NRMSD 3.68 shows the highest deviation, indicating a large discrepancy in wet day estimations, whereas ACCESS-ESM-1.5 with 1.04 exhibits the lowest deviation, suggesting a relatively better alignment with observations. For Station 808, INM-CM4.8 with 2.30 and MRI-ESM2.0 with NRMSD 2.42 show higher deviations, while EC-EARTH3-VEG having NRMSD 0.69 performs best with the lowest deviation. At Station 1004, INM-CM4.8 with NRMSD 0.01 has an exceptionally low NMRSD, implying a near-perfect match with observations, whereas ACCESS-ESM-1.5 with 1.57 and MIROC6 with 1.09 exhibit moderate deviations. MPI-ESM1.2-LR and NESM3 show varying performances across stations, with generally lower deviations at Station 1004 compared to others. Overall, INM-CM4.8 shows extreme variability, performing worst at Station 804 but excelling at Station 1004, while EC-EARTH3-VEG and ACCESS-ESM-1.5 demonstrate more consistent performance across stations.

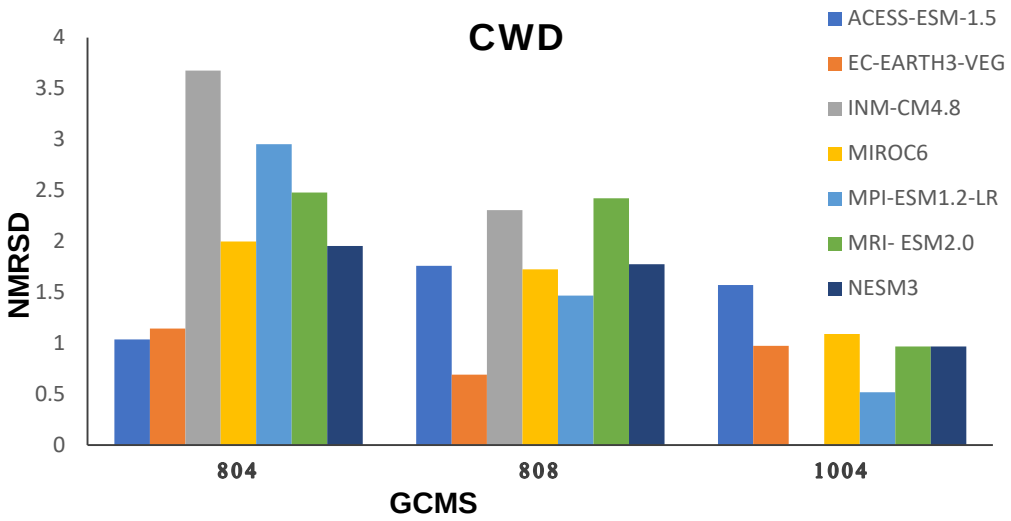

Figure 5-5 Variation of NRMSD for the CWD index across different stations.

The Normalized Root Mean Square values for R10 across different GCMs show relatively lower deviations compared to DHM observations, indicating better model performance in capturing heavy rainfall events. At Station 804, INM-CM4.8 with NRMSD 0.12 has the lowest deviation, suggesting the best agreement with observations, while MIROC6 has 0.24 shows the highest deviation. At Station 808, EC-EARTH3-VEG having value 0.22, MPI-ESM1.2-LR with value 0.28 and NESM3 with 0.22 perform similarly, with ACCESS-ESM-1.5 with 0.34 having the highest deviation. For Station 1004, EC-EARTH3-VEG with 0.15 has the best performance, while ACCESS-ESM-1.5 with 0.30 shows the highest discrepancy. Across all stations, EC-EARTH3-VEG and INM-CM4.8 generally exhibit the lowest deviations, making them the most reliable models for simulating heavy precipitation days, while ACCESS-ESM-1.5 and MIROC6 show relatively higher deviations.

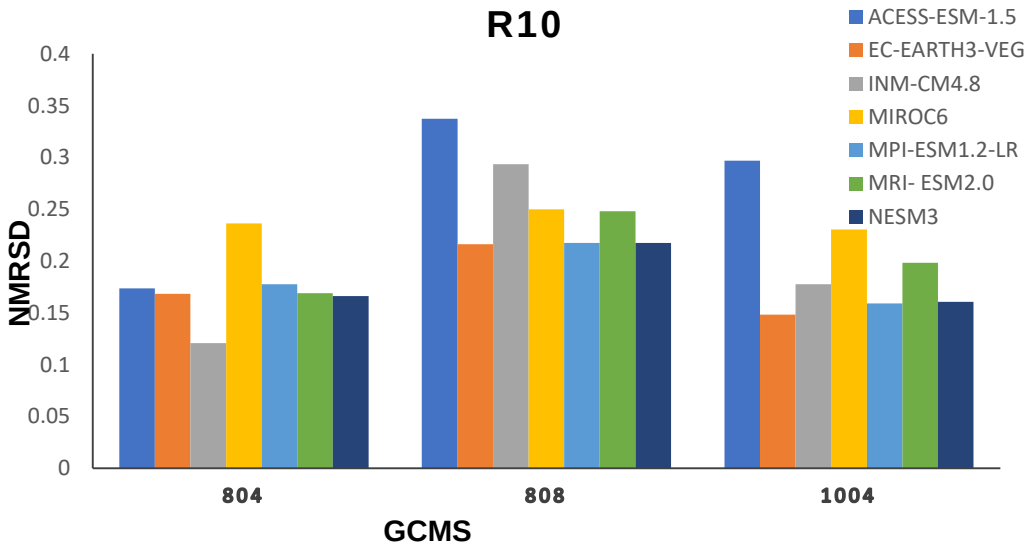

Figure 5-6 Variation of NRMSD for the R10 index across different stations.

5.2.3 Absolute normalized root mean square

The Absolute Normalized Root Mean Square Difference values for Consecutive Dry Days across different GCMs indicate variations in model performance when compared to DHM observations. At Station 804, ACCESS-ESM-1.5 with NRMSD 0.04 and NESM3 with 0.07 have the lowest deviations, suggesting better alignment with observed data, while INM-CM4.8 having 0.59 shows the highest deviation. For Station 808, EC-EARTH3-VEG with 0.03 exhibits the best agreement with observations, whereas NESM3 has 0.37 and MRI-ESM2.0 with 0.33 have relatively higher deviations. At Station 1004, NESM3 having 0.05 and MPI-ESM1.2-LR with 0.06 show the least deviation, making them the most reliable for capturing dry spell variations, while ACCESS-ESM-1.5 with 0.26 presents the highest discrepancy. Overall, EC-EARTH3-VEG, NESM3 and MPI-ESM1.2-LR tend to exhibit lower deviations, making them more reliable in simulating consecutive dry days, while INM-CM4.8 consistently shows higher discrepancies, indicating weaker performance.

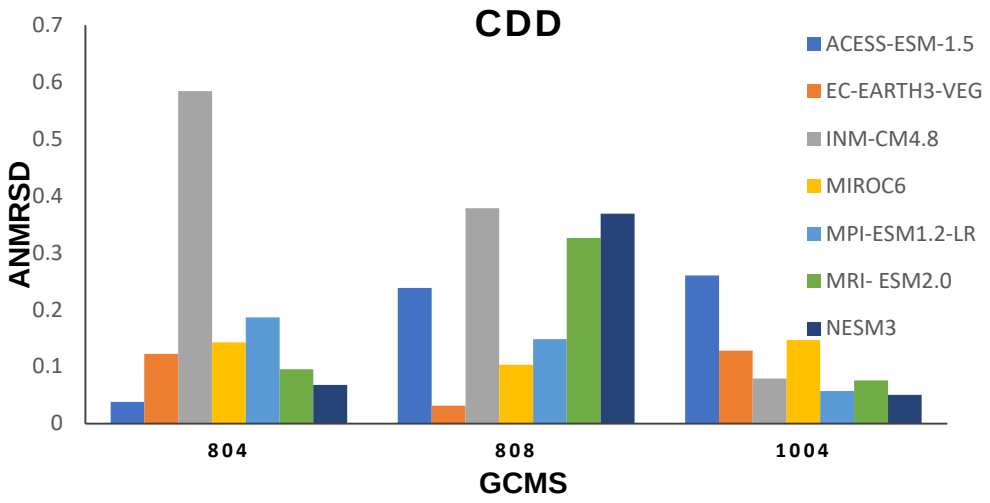

Figure 5-7 Variation of ANRMSD for the CDD index across different stations.

The Absolute Normalized Root Mean Square Difference values for Consecutive Wet Days across different GCMs reveal significant variations in model performance when compared to DHM observations. At Station 804, ACCESS-ESM-1.5 with ANRMSD 0.61 and EC-EARTH3-VEG with 0.85 show the lowest deviations, making them the most reliable models, while INM-CM4.8 with 3.60 exhibits the highest discrepancy. For Station 808, EC-EARTH3-VEG with 0.56 and MPI-ESM1.2-LR with 1.30 perform relatively well, whereas INM-CM4.8 having 2.10 and MRI-ESM2.0 having 2.15 show larger deviations. At Station 1004, MPI-ESM1.2-LR with 0.06 has the smallest deviation, followed by NESM3 with 0.58 and MIROC6 with 0.552, while INM-CM4.8 with 0.25 and ACCESS-ESM-1.5 with 0.92 show greater discrepancies. Overall, EC-EARTH3-VEG, NESM3 and MPI-ESM1.2-LR demonstrate better agreement with observations for consecutive wet days, whereas INM-CM4.8 consistently exhibits the highest deviation, indicating weaker performance in capturing wet spells.

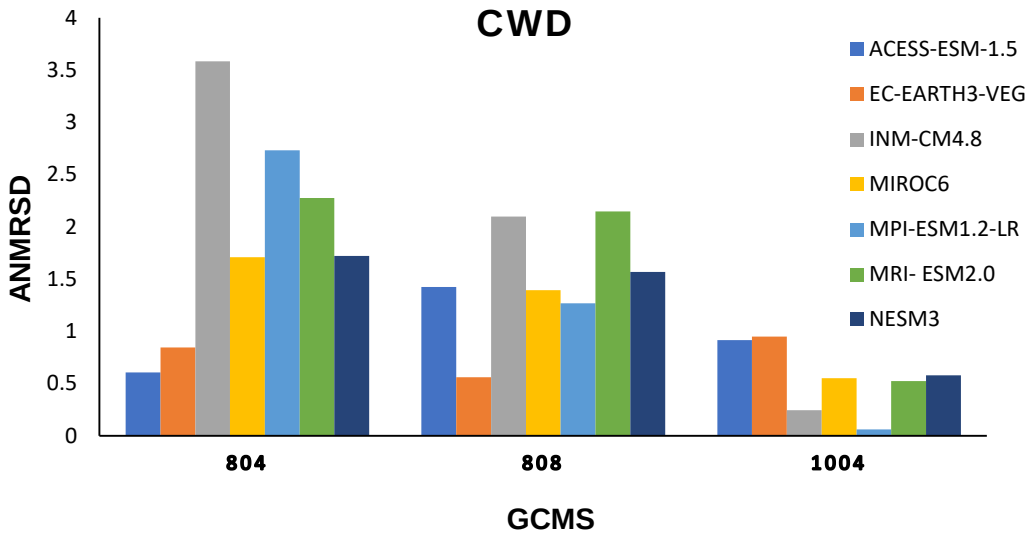

Figure 5-8 Variation of ANRMSD for the CWD index across different stations.

The Absolute Normalized Root Mean Square Deviation values for R10 across different GCMs indicate relatively low deviations from DHM observations, suggesting better model performance compared to CWD and CDD. At Station 804, ACCESS-ESM-1.5 with ANRMSD 0.00 exhibits an exceptionally low deviation, making it the best-performing model, while the other models range between 0.11 for MIROC6 and 0.1208 for INM-CM4.8. For Station 808, deviations are slightly higher, with ACCESS-ESM-1.5 with 0.01 again showing the lowest value, followed by EC-EARTH3-VEG having 0.15 and MPI-ESM1.2-LR with 0.16, whereas INM-CM4.8 with 0.17 has the highest deviation. At Station 1004, MIROC6 has 0.04 and INM-CM4.8 has 0.04 show the lowest deviations, while ACCESS-ESM-1.5 having 0.00 remains the most accurate. Overall, ACCESS-ESM-1.5 consistently exhibits the lowest deviations across all stations, suggesting superior performance in capturing the frequency of heavy rainfall days, while INM-CM4.8 and MRI-ESM2.0 show slightly larger discrepancies.

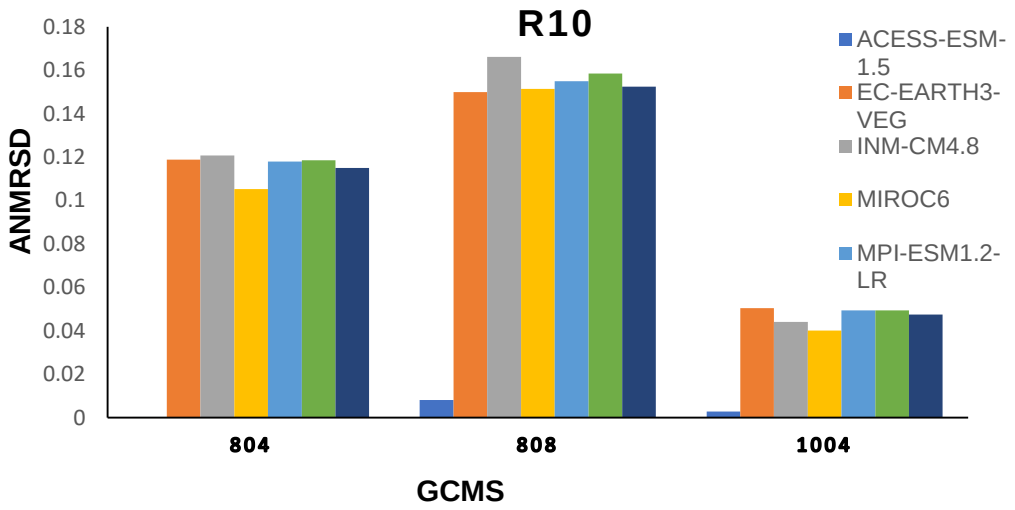

Figure 5-9 Variation of ANRMSD for the R10 index across different stations.

5.2.4 Average absolute relative deviation

The Average Absolute Relative Deviation values for Consecutive Dry Days across different GCMs show varying degrees of deviation from DHM observations, with some models performing better than others across different stations. At Station 804, INM-CM4.8 having value 0.82 exhibits the highest deviation, indicating a weaker representation of dry spell durations, whereas MRI-ESM2.0 with 0.29 and NESM3 with 0.30 show the lowest deviations, suggesting a relatively better performance. For Station 808, ACCESS-ESM-1.5 having value of 0.34, MPI-ESM1.2-LR having value 0.32 and EC-EARTH3-VEG with 0.2487 have moderate deviations, but NESM3 with 0.43 shows a relatively higher discrepancy. At Station 1004, INM-CM4.8 with 0.17 has the lowest deviation, while NESM3 with 0.28 and MPI-ESM1.2-LR with 0.27 show slightly higher deviations. Overall, INM-CM4.8 exhibits high deviation at Station 804 but performs best at Station 1004, while MRI-ESM2.0 and NESM3 consistently show lower deviations, making them potentially more reliable in simulating dry spell durations.

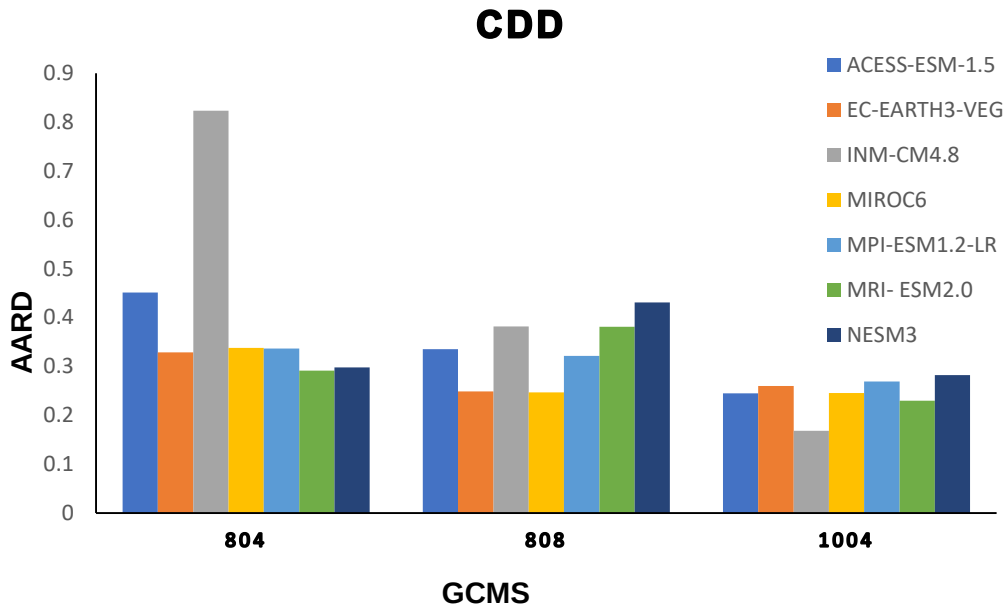

Figure 5-10 Variation of AARD for the CDD index across different stations

The Average Absolute Relative Deviation values for Consecutive Wet Days across different GCMs show significant variability, indicating differing levels of agreement with DHM observations. At Station 804, INM-CM4.8 with AARD as 2.77 has the highest deviation, suggesting a weaker simulation of wet spell durations, while ACCESS-ESM-1.5 with 0.43 and EC-EARTH3-VEG with 0.69 show relatively lower deviations, making them more reliable for this station. At Station 808, MRI-ESM2.0 with 2.99 and INM-CM4.8 with 2.93 exhibit the highest deviations, whereas EC-EARTH3-VEG with 0.79 and MPI-ESM1.2-LR with 1.77 perform moderately well. For Station 1004, MPI-ESM1.2-LR with 0.25 and INM-CM4.8 with 0.26 have the lowest deviations, indicating good agreement with observations, while EC-EARTH3-VEG having 0.54 and NESM3 having 0.42 show slightly higher deviations. Overall, ACCESS-ESM-1.5 and EC-EARTH3-VEG perform better at Station 804, while MPI-ESM1.2-LR and INM-CM4.8 show the best agreement at Station 1004. However, high deviations at Station 808 for multiple models suggest challenges in accurately capturing wet spell durations in that region.

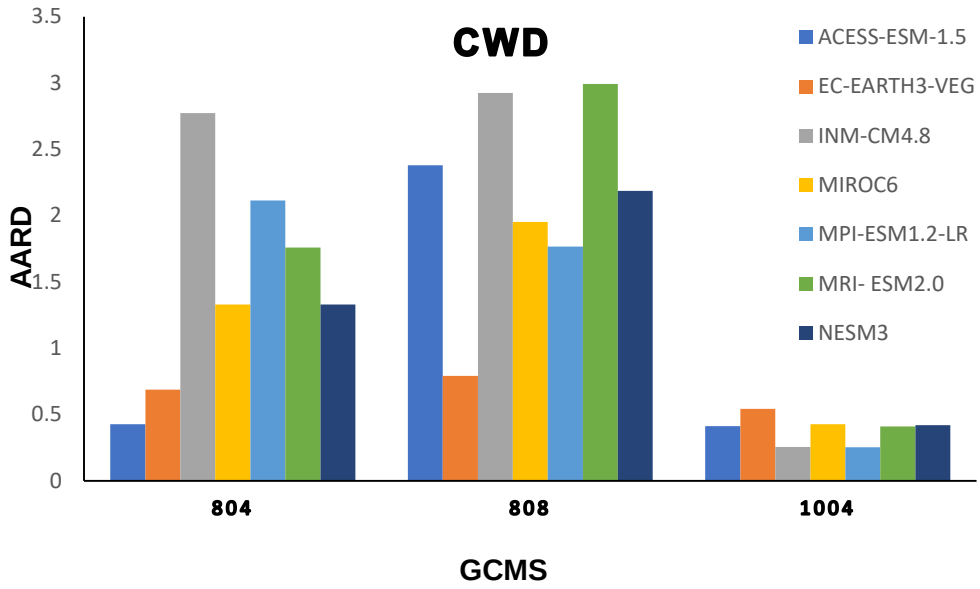

Figure 5-11 Variation of AARD for the CWD index across different stations

The Average Absolute Relative Deviation values for R10 across different GCMs indicate relatively lower deviations compared to CDD and CWD, suggesting better model agreement with DHM observations for extreme precipitation. At Station 804, EC-EARTH3-VEG with 0.11 and MRI-ESM2.0 with 0.12 have the lowest deviations, indicating strong agreement with observed data, while MIROC6 with 0.16 and INM-CM4.8 with 0.15 show slightly higher deviations. At Station 808, MPI-ESM1.2-LR with 0.21 and NESM3 with 0.21 have relatively lower deviations, whereas INM-CM4.8 having 0.28 shows the highest deviation, suggesting potential challenges in simulating extreme precipitation events at this location. At Station 1004, EC-EARTH3-VEG has value of 0.17 exhibits the lowest deviation, followed by MPI-ESM1.2-LR having the value of 0.13 and NESM3 with value of 0.13, while MIROC6 has 0.17 has the highest deviation. Overall, EC-EARTH3-VEG and MRI-ESM2.0 perform best at Station 804, while EC-EARTH3-VEG and MPI-ESM1.2-LR show the highest agreement at Station 1004. INM-CM4.8 exhibits the highest deviation at Station 808, suggesting limitations in capturing extreme precipitation trends in that region.

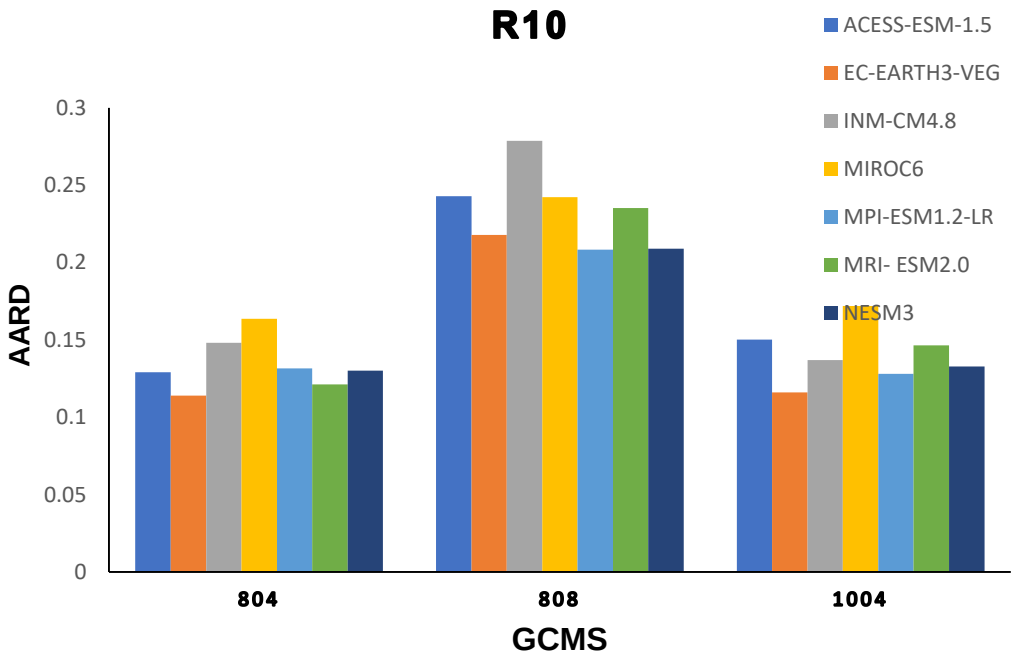

Figure 5-12 Variation of AARD for the R10 index across different stations

5.3 Ranking of the GCMs

Ranking of GCMs was done by using the technique of comprise programming. For this study comprise programming refers to the overall ability of a general circulation model to realistically simulate essential climate indices CDD, CWD and R10 both over time and across different regions. It involves evaluating the model's accuracy using statistical measures like CC, NRMSD, ANRMSD and AARD, as well as its skill in capturing seasonal patterns and long-term climate trends. A model with strong comprise programming performs consistently well in reproducing observed climate data and is therefore considered reliable for regional climate analysis and future climate projections.

At Station 804: The ranking of seven GCMs based on three climate indices CDD, CWD, and R10 at highlights varying model performances .EC-EARTH3-VEG ranks first in CDD-prolonged dry periods, but last in R10 -heavy rainfall days, suggesting strong drought simulation but potential underestimation of extreme rainfall . NESM3 performs well in CWD)1st (and R10)3rd(, indicating reliability in wet conditions .MIROC6 is the most consistent, ranking 2nd in all indices, making it a

balanced model .MRI-ESM2.0 and ACCESS-ESM1.5 show mixed rankings, performing moderately across indices .MPI-ESM1.2-LR and INM-CM4.8 generally rank lower, with INM-CM4.8 being last in CDD and among the lowest in R10, suggesting weaker performance in simulating dry and extreme rainfall events . These rankings indicate that different models excel in different climate conditions, and MIROC6 emerges as a well-rounded choice.

Table 5-13 Ranking of 7 GCMs by three climate indices in the station 804

Rank	**CDD**	**CWD**	**R10**
1	EC-EARTH3-VEG	NESM3	ACESS-ESM-1.5
2	MIROC6	MIROC6	MIROC6
3	NESM3	MRI- ESM2.0	NESM3
4	MRI- ESM2.0	EC-EARTH3-VEG	MPI-ESM1.2-LR
5	ACESS-ESM-1.5	INM-CM4.8	MRI- ESM2.0
6	MPI-ESM1.2-LR	ACESS-ESM-1.5	INM-CM4.8
7	INM-CM4.8	MPI-ESM1.2-LR	EC-EARTH3-VEG

At Station 808: MIROC6 ranks 1st in CDD but falls to 6th in R10, indicating strong drought simulation but potential underestimation of extreme rainfall events .EC-EARTH3-VEG performs best in CWD and 2nd in R10, suggesting reliability in capturing wet periods and heavy rainfall .MPI-ESM1.2-LR shows consistency, ranking 2nd in CDD and CWD and 3rd in R10, making it a well-balanced model . ACCESS-ESM1.5 ranks 1st in R10 and 4th in the other indices, indicating a strength in heavy rainfall simulation. MRI-ESM2.0 and NESM3 exhibit mid-to-lower rankings across all indices, while INM-CM4.8 ranks lowest in R10 and CWD, suggesting weaker performance in wet conditions .Overall, MIROC6 and EC-EARTH3-VEG perform well in dry and wet extremes, respectively, while MPI-ESM1.2-LR emerges as a balanced choice across all indices।

Table 5-14 Ranking of 7 GCMs by three climate indices in the station 808

Rank	CDD	CWD	R10
1	MIROC6	EC-EARTH3-VEG	ACESS-ESM-1.5
2	MPI-ESM1.2-LR	MPI-ESM1.2-LR	EC-EARTH3-VEG
3	EC-EARTH3-VEG	MIROC6	MPI-ESM1.2-LR
4	ACESS-ESM-1.5	ACESS-ESM-1.5	NESM3
5	MRI- ESM2.0	NESM3	MRI- ESM2.0
6	INM-CM4.8	INM-CM4.8	MIROC6
7	NESM3	MRI- ESM2.0	INM-CM4.8

At station 1004: INM-CM4.8 ranks 1st in both CDD and CWD, suggesting strong capabilities in simulating both dry and wet spell durations, while it also performs well in R10 being on rank 2nd, making it the most balanced model .ACCESS-ESM1.5 ranks 1st in R10 but 6th in CDD and 7th in CWD, indicating strength in capturing heavy rainfall events but potential weaknesses in representing prolonged dry and wet periods .MRI-ESM2.0 ranks consistently in the upper half for CDD with 2nd and CWD having rank 3rd but drops to 7th in R10, suggesting it models dry and wet durations well but underestimates extreme rainfall .NESM3 and MPI-ESM1.2-LR hold mid-tier rankings across all indices, showing moderate performance .EC-EARTH3-VEG and MIROC6 rank lower in most indices, withMIROC6 performing the worst in CDD with rank 7th but moderately in R10 with 3rd rank .Overall, NM-CM4.8 emerges as the strongest performer across all indices, while ACCESS-ESM1.5 specializes in extreme rainfall, and MRI-ESM2.0 is reliable for dry and wet durations but less so for heavy rain.

Table 5-15 Ranking of 7 GCMs by three climate indices in the station 1004

Rank	**CDD**	**CWD**	**R10**
1	INM-CM4.8	INM-CM4.8	ACESS-ESM-1.5
2	MRI- ESM2.0	MPI-ESM1.2-LR	INM-CM4.8
3	NESM3	MRI- ESM2.0	MIROC6
4	MPI-ESM1.2-LR	NESM3	NESM3
5	EC-EARTH3-VEG	MIROC6	MPI-ESM1.2-LR
6	ACESS-ESM-1.5	EC-EARTH3-VEG	EC-EARTH3-VEG
7	MIROC6	ACESS-ESM-1.5	MRI- ESM2.0

6 C0NCLUSION

6.1 Summary of Findings

This study evaluated the performance of selected CMIP6 general circulation models (GCMs) in simulating extreme precipitation indices across the Central Hill Region of Nepal, focusing on an elevation range of 800 to 1000 meters. Using three key climate indices, Consecutive Dry Days, Consecutive Wet Days, and the number of heavy precipitation days along with multiple statistical performance metrics, the results revealed that no single model consistently outperformed others across all indices and stations. However, MIROC6 showed the most consistent performance with relatively low deviations across different indices and locations.

- For the CDD index, EC-EARTH3-VEG ranked as the top performer, followed closely by MIROC6, while ACCESS-ESM-1.5 exhibited the weakest performance.
- For the CWD index, NESM3 and MIROC6 were identified as the best-performing models, with EC-EARTH3-VEG ranking second, and ACCESS-ESM-1.5 again showing the poorest performance.
- For the R10 index, ACCESS-ESM-1.5 performed best overall, followed by MIROC6 and NESM3, whereas MRI-ESM2.0 ranked the lowest.

The evaluated CMIP6 models can therefore be used for climate studies in the Central Hill Region of Nepal; however, model selection should be done carefully based on the specific climate index and study location. Models such as MIROC6, EC-EARTH3-VEG, and NESM3 are particularly suitable for selected extreme precipitation indices for that particular region. To improve reliability and account for model uncertainties, a multi-model ensemble approach is recommended.

Despite providing important insights, this study had some limitations, including the use of only three stations, a focus on only three precipitation-based indices, and reliance on historical simulations without projecting future climate conditions under different SSP-RCP scenarios. Nevertheless, the findings emphasize that region-specific model evaluation is crucial for enhancing the accuracy of climate impact studies, and they provide a strong foundation for guiding future adaptation and policy strategies in Nepal's Central Hill Region.

6.2 Recommendations for Future Works

Based on the findings of this study, several recommendations are proposed to improve the reliability and applicability of climate model evaluations for the Central Hill Region of Nepal.

Firstly, future studies should incorporate multiple SSP-RCP scenarios to analyze the models' performance under a range of future climate conditions. Comparative assessment across different emission pathways would enhance the relevance and applicability of model rankings for long-term climate impact studies and adaptation planning.

Secondly, expanding the number of meteorological stations and extending the temporal coverage of observational data would help capture greater spatial and climatic variability across the region. This would strengthen the robustness and representativeness of the evaluation, particularly in diverse terrains like Nepal's mid-hills.

Thirdly, including a broader set of extreme climate indices, such as temperature extremes and other precipitation-related indicators, would provide a more comprehensive assessment of model capabilities. Future research should also evaluate future projections, not only historical simulations, to assess the models' ability to predict climate extremes under changing conditions.

Finally, adopting a multi-model ensemble approach is strongly recommended, as it can reduce uncertainties associated with individual model biases and provide a more reliable basis for decision-making in climate-sensitive sectors such as agriculture, water resources, and disaster risk management.

6.3 Policy Implications

The findings of this study hold important implications for policy-making in the context of climate change adaptation, water resource management, and disaster risk reduction in Nepal, particularly within the mid hills of central Nepal. By identifying which climate models most accurately simulate extreme weather events such as prolonged dry spells, sustained wet periods, and heavy rainfall days this research provides a scientific basis for improving climate-informed decision-making at both regional and national levels.

First, the ability to accurately simulate extreme climate events is crucial for designing effective early warning systems, disaster preparedness plans, and resilient infrastructure. For instance, reliable projections of heavy rainfall events can support better planning of flood defenses, riverbank protection, and urban drainage systems in downstream areas like Pokhara, which are prone to monsoon-related flooding. Similarly, information on consecutive dry days is essential for drought preparedness, agricultural planning, and ensuring water availability during dry seasons.

Second, the study supports the use of a multi-model ensemble approach, which can reduce uncertainties in climate projections. This insight encourages policy-makers to base long-term strategies on robust climate information derived from multiple validated models, rather than relying on a single model. This can be particularly beneficial in formulating national adaptation plans (NAPs), local adaptation plans for action (LAPAs), and integrated river basin management strategies.

Third, the research provides a replicable evaluation framework for climate model selection, which can be applied to other river basins or districts across Nepal. This contributes to the development of regionally tailored policies, enhancing the accuracy of climate risk assessments and the efficiency of climate finance allocation.

Finally, by promoting science-based model selection, the study strengthens the link between research and policy. Government agencies like the Department of Hydrology and Meteorology (DHM), the Ministry of Forests and Environment (MoFE), and local municipalities can incorporate these findings to update hazard maps, revise building codes, and support climate-resilient development initiatives.

In conclusion, this research provides actionable insights that can guide evidence-based policy decisions, contributing to a more resilient and climate-adaptive future for communities.

REFERENCES

Altamirano del Carmen, M. A., Estrada, F., & Gay-García, C. (2021). A new method for assessing the performance of general circulation models based on their ability to simulate the response to observed forcing. *Journal of Climate*, *34*(13), 5385–5402.

Baghel, T., Babel, M. S., Shrestha, S., Salin, K. R., Virdis, S. G., & Shinde, V. R. (2022a). A generalized methodology for ranking climate models based on climate indices for sector-specific studies: An application to the Mekong sub-basin. *Science of The Total Environment*, *829*, 154551.

Baghel, T., Babel, M. S., Shrestha, S., Salin, K. R., Virdis, S. G., & Shinde, V. R. (2022b). A generalized methodology for ranking climate models based on climate indices for sector-specific studies: An application to the Mekong sub-basin. *Science of The Total Environment*, *829*, 154551.

Balaji, V., Taylor, K. E., Juckes, M., Lawrence, B. N., Durack, P. J., Lautenschlager, M., Blanton, C., Cinquini, L., Denvil, S., & Elkington, M. (2018). Requirements for a global data infrastructure in support of CMIP6. *Geoscientific Model Development*, *11*(9), 3659–3680.

Bhuyan, D. P., Salunke, P., & Chadha, M. (2024). Climate projections for Himalaya–Tibetan Highland. *Theoretical and Applied Climatology*, *155*(2), 1055–1065. https://doi.org/10.1007/s00704-023-04677-w

Borgomeo, E. (2022). Water Resource System Modelling for Climate Adaptation. In *Climate Adaptation Modelling* (pp. 141–147). Springer International Publishing Cham. https://library.oapen.org/bitstream/handle/20.500.12657/60795/978-3-030-86211-4.pdf?sequence=1#page=148

Change, I. (2007). Climate change 2007: The physical science basis. *Agenda*, *6*(07), 333.

Dahal, P., Shrestha, M. L., Panthi, J., & Pradhananga, D. (2020a). Modeling the future impacts of climate change on water availability in the Karnali River Basin of Nepal Himalaya. *Environmental Research*, *185*, 109430.

Dahal, P., Shrestha, M. L., Panthi, J., & Pradhananga, D. (2020b). Modeling the future impacts of climate change on water availability in the Karnali River Basin of Nepal Himalaya. *Environmental Research*, *185*, 109430.

Daramola, M. T., & Xu, M. (2022). Recent changes in global dryland temperature and precipitation. *International Journal of Climatology*, *2*, 1267–1282.

Dey, A., Sahoo, D. P., Kumar, R., & Remesan, R. (2022). A multimodel ensemble machine learning approach for CMIP6 climate model projections in an Indian River basin. *International Journal of Climatology*, *42*(16), 9215–9236.

Dhital, H. P., Joshi, M., & Budhathoki, N. (2023). Impacts of Climate Change on Temperature and Precipitation in Nepal: Projections and Bias Correction. *Journal of Sustainability and Environmental Management*, *2*(4), 203–212.

DHM (2017). Observational Climate Data of Nepal (1981–2010). Department of Hydrology and Meteorology, Government of Nepal. - Google Search. (n.d.). Retrieved 26 April 2025, from https://www.google.com/search?q=DHM+(2017).+Observational+Climate+Data+of+Nepal+(1981%E2%80%932010).+Department+of+Hydrology+and+Meteorology%2C+Government+of+Nepal.&rlz=1C1KNTJ_enNP1066NP1072&oq=DHM+(2017).+Observational+Climate+Data+of+Nepal+(1981%E2%80%932010).+Department+of+Hydrology+and+Meteorology%2C+Government+of+Nepal.&gs_lcrp=EgZjaHJvbWUyBggAEEUYOTIGCAEQRRg8MgYIAhBFGDzSAQkyNzYzajBqMTWoAgiwAgHxBVfDmr0CmzAu8QVXw5q9ApswLg&sourceid=chrome&ie=UTF-8

Dix, M., Bi, D., Dobrohotoff, P., Fiedler, R., Harman, I., Law, R., Mackallah, C., Marsland, S., O'Farrell, S., & Rashid, H. (2019). *CSIRO-ARCCSS access-CM2 model output prepared for CMIP6 CMIP 1pctco2*. https://www.wdc-climate.de/ui/entry?acronym=C6_4381093

Donat, M. G., Alexander, L. V., Yang, H., Durre, I., Vose, R., Dunn, R. J. H., Willett, K. M., Aguilar, E., Brunet, M., Caesar, J., Hewitson, B., Jack, C., Klein Tank, A. M. G., Kruger, A. C., Marengo, J., Peterson, T. C., Renom, M., Oria Rojas, C., Rusticucci, M., … Kitching, S. (2013). Updated analyses of temperature and precipitation extreme indices since the beginning of the twentieth century: The HadEX2 dataset. *Journal of Geophysical Research: Atmospheres*, *118*(5), 2098–2118. https://doi.org/10.1002/jgrd.50150

Ehret, U., Zehe, E., Wulfmeyer, V., & Liebert, J. (2012). *Should we apply bias correction to global and regional climate model data? HESS, 16, 3391–3404*.

ETCCDI. (2009). Guidelines on analysis of extremes in a changing climate in support of informed decisions for adaptation. Geneva, Switzerland.

Eyring, V., Bony, S., Meehl, G. A., Senior, C. A., Stevens, B., Stouffer, R. J., & Taylor, K. E. (2016a). Overview of the Coupled Model Intercomparison Project Phase 6 (CMIP6) experimental design and organization. *Geoscientific Model Development*, *9*(5), 1937–1958.

Eyring, V., Bony, S., Meehl, G. A., Senior, C. A., Stevens, B., Stouffer, R. J., & Taylor, K. E. (2016b). Overview of the Coupled Model Intercomparison Project Phase 6 (CMIP6) experimental design and organization. *Geoscientific Model Development*, *9*(5), Article 5.

Gao, W., Li, J., Cheng, D., Liu, L., Liu, J., Le, T. D., Du, X., Chen, X., Zhao, Y., & Chen, Y. (2024). *A Deconfounding Approach to Climate Model Bias Correction* (No. arXiv:2408.12063). arXiv. https://doi.org/10.48550/arXiv.2408.12063

Gómez, M. J., Barboza, L. A., Hidalgo, H. G., & Alfaro, E. J. (2023). *Comparison of indicators to evaluate the performance of climate models* (No. arXiv:2307.04658). arXiv. https://doi.org/10.48550/arXiv.2307.04658

Gudmundsson, L., Bremnes, J. B., Haugen, J. E., & Engen-Skaugen, T. (2012). Downscaling RCM precipitation to the station scale using statistical transformations–a comparison of methods. *Hydrology and Earth System Sciences*, *16*(9), 3383–3390.

Gumus, B., Oruc, S., Yucel, I., & Yilmaz, M. T. (2023). Impacts of climate change on extreme climate indices in Türkiye driven by high-resolution downscaled CMIP6 climate models. *Sustainability*, *15*(9), 7202.

Haarsma, R. J., Roberts, M. J., Vidale, P. L., Senior, C. A., Bellucci, A., Bao, Q., Chang, P., Corti, S., Fučkar, N. S., & Guemas, V. (2016). High resolution model intercomparison project (HighResMIP v1. 0) for CMIP6. *Geoscientific Model Development*, *9*(11), 4185–4208.

Harrison, P. A., Holman, I. P., & Berry, P. M. (2015). Assessing cross-sectoral climate change impacts, vulnerability and adaptation: An introduction to the CLIMSAVE project. *Climatic Change*, *128*(3), 153–167. https://doi.org/10.1007/s10584-015-1324-3

Hegerl, G. C., Brönnimann, S., Schurer, A., & Cowan, T. (2018). The early 20th century warming: Anomalies, causes, and consequences. *WIREs Climate Change*, *9*(4), e522. https://doi.org/10.1002/wcc.522

Hess, P., Lange, S., Schötz, C., & Boers, N. (2023). Deep Learning for Bias-Correcting CMIP6-Class Earth System Models. *Earth's Future*, *11*(10), e2023EF004002. https://doi.org/10.1029/2023EF004002

Hulme, M., Mitchell, J., Ingram, W., Lowe, J., Johns, T., New, M., & Viner, D. (1999). Climate change scenarios for global impacts studies. *Global Environmental Change*, *9*, S3–S19. https://doi.org/10.1016/S0959-3780(99)00015-1

ICIMOD (2010). Climate change vulnerability of mountain ecosystems in the Eastern Himalayas. International Centre for Integrated Mountain Development. - Google Search. (n.d.). Retrieved 26 April 2025, from https://www.google.com/search?q=ICIMOD+(2010).+Climate+change+vulnerability+of+mountain+ecosystems+in+the+Eastern+Himalayas.+International+Centre+for+Integrated+Mountain+Development.&rlz=1C1KNTJ_enNP1066NP1072&oq=ICIMOD+(2010).+Climate+change+vulnerability+of+mountain+ecosystems+in+the+Eastern+Himalayas.+International+Centre+for+Integrated+Mountain+Development.&gs_lcrp=EgZjaHJvbWUyBggAEEUYOdIBCTIxMTBqMGoxNagCCLACAfEFPABnxlW5I1jxBTwAZ8ZVuSNY&sourceid=chrome&ie=UTF-8

Kebede, A. S., Nicholls, R. J., Allan, A., Arto, I., Cazcarro, I., Fernandes, J. A., Hill, C. T., Hutton, C. W., Kay, S., Lázár, A. N., Macadam, I., Palmer, M., Suckall, N., Tompkins, E. L., Vincent, K., & Whitehead, P. W. (2018a). Applying the global RCP–SSP–SPA scenario framework at sub-national scale: A multi-scale and participatory scenario approach. *Science of The Total Environment*, *635*, 659–672. https://doi.org/10.1016/j.scitotenv.2018.03.368

Kebede, A. S., Nicholls, R. J., Allan, A., Arto, I., Cazcarro, I., Fernandes, J. A., Hill, C. T., Hutton, C. W., Kay, S., Lázár, A. N., Macadam, I., Palmer, M., Suckall, N., Tompkins, E. L., Vincent, K., & Whitehead, P. W. (2018b). Applying the global RCP–SSP–SPA scenario framework at sub-national scale: A multi-scale and participatory scenario approach. *Science of The Total Environment*, *635*, 659–672. https://doi.org/10.1016/j.scitotenv.2018.03.368

Kim, Y.-T., Yu, J.-U., Kim, T.-W., & Kwon, H.-H. (2024). A novel approach to a multi-model ensemble for climate change models: Perspectives on the representation of natural variability and historical and future climate. *Weather and Climate Extremes*, *44*, 100688.

Kriegler, E., Edmonds, J., Hallegatte, S., Ebi, K. L., Kram, T., Riahi, K., Winkler, H., & van Vuuren, D. P. (2014). A new scenario framework for climate change research: The concept of shared climate policy assumptions. *Climatic Change*, *122*(3), 401–414. https://doi.org/10.1007/s10584-013-0971-5

Lawrence, D. M., Hurtt, G. C., Arneth, A., Brovkin, V., Calvin, K. V., Jones, A. D., Jones, C. D., Lawrence, P. J., de Noblet-Ducoudré, N., & Pongratz, J. (2016). The Land Use Model Intercomparison Project (LUMIP) contribution to CMIP6: Rationale and experimental design. *Geoscientific Model Development*, *9*(9), 2973–2998.

Lazoglou, G., Economou, T., Anagnostopoulou, C., Tzyrkalli, A., Zittis, G., & Lelieveld, J. (2024). Bias correction of daily precipitation from climate models, using the Q-GAM method. *Environmetrics*, *35*(7), e2881. https://doi.org/10.1002/env.2881

Liu, J., Yuan, F., Zuo, Y., Zhou, R., Zhu, X., Li, K., Wang, N., Chen, N., Guo, Z., & Zhang, L. (2022). Warming-induced vegetation growth cancels out soil carbon-climate feedback in the northern Asian permafrost region in the 21st century. *Environmental Research Letters*, *17*(8), 084009.

Manikanta, V., Reddy, V. M., & Das, J. (2024). Investigating the Limitations of Multi-Model Ensembling of Climate Model Outputs in Capturing Climate Extremes. *International Journal of Climatology*, *44*(16), 5711–5726. https://doi.org/10.1002/joc.8660

Maraun, D. (2016). Bias Correcting Climate Change Simulations—A Critical Review. *Current Climate Change Reports*, *2*(4), 211–220. https://doi.org/10.1007/s40641-016-0050-x

Masson-Delmotte, V. P., Zhai, P., Pirani, S. L., Connors, C., Péan, S., Berger, N., Caud, Y., Chen, L., Goldfarb, M. I., & Scheel Monteiro, P. M. (2021). *Ipcc, 2021: Summary for policymakers. in: Climate change 2021: The physical science basis. contribution of working group i to the sixth assessment report of the intergovernmental panel on climate change*. http://researchspace.csir.co.za/dspace/handle/10204/12710

Meehl, G. A., Boer, G. J., Covey, C., Latif, M., & Stouffer, R. J. (1997). Intercomparison makes for a better climate model. *Eos, Transactions American Geophysical Union*, *78*(41), 445–451. https://doi.org/10.1029/97EO00276

Mishra, V., Bhatia, U., & Tiwari, A. D. (2020). Bias-corrected climate projections for South Asia from Coupled Model Intercomparison Project-6. *Scientific Data*, *7*(1), 338. https://doi.org/10.1038/s41597-020-00681-1

Moss: The next generation of scenarios for climate... - Google Scholar. (n.d.). Retrieved 17 August 2024, from https://scholar.google.com/scholar_lookup?title=The%20next%20generation%20of%20scenarios%20for%20climate%20change%20research%20and%20assessment&publication_year=2010&author=R.H.%20Moss&author=J.A.%20Edmonds&author=K.A.%20Hibbard

Myhre, G., Aas, W., Cherian, R., Collins, W., Faluvegi, G., Flanner, M., Forster, P., Hodnebrog, Ø., Klimont, Z., & Lund, M. T. (2017). Multi-model simulations of aerosol and ozone radiative forcing due to anthropogenic emission changes during the period 1990–2015. *Atmospheric Chemistry and Physics*, *17*(4), 2709–2720.

Neupane, J. L. (2022). *Dynamics of Hydro-power Development in Nepal: Water-Energy-Food Security Prospect*. https://www.diva-portal.org/smash/record.jsf?pid=diva2:1665598

Ngai, S. T., Tangang, F., & Juneng, L. (2017). Bias correction of global and regional simulated daily precipitation and surface mean temperature over Southeast Asia using quantile mapping method. *Global and Planetary Change*, *149*, 79–90.

O'Neill, B. C., Carter, T. R., Ebi, K., Harrison, P. A., Kemp-Benedict, E., Kok, K., Kriegler, E., Preston, B. L., Riahi, K., Sillmann, J., van Ruijven, B. J., van Vuuren, D., Carlisle, D., Conde, C., Fuglestvedt, J., Green, C., Hasegawa, T., Leininger, J., Monteith, S., & Pichs-Madruga, R. (2020a). Achievements and needs for the climate change scenario framework. *Nature Climate Change*, *10*(12), 1074–1084. https://doi.org/10.1038/s41558-020-00952-0

O'Neill, B. C., Carter, T. R., Ebi, K., Harrison, P. A., Kemp-Benedict, E., Kok, K., Kriegler, E., Preston, B. L., Riahi, K., Sillmann, J., van Ruijven, B. J., van Vuuren, D., Carlisle, D., Conde, C., Fuglestvedt, J., Green, C., Hasegawa, T., Leininger, J., Monteith, S., & Pichs-Madruga, R. (2020b). Achievements and needs for the climate change scenario framework. *Nature Climate Change*, *10*(12), Article 12. https://doi.org/10.1038/s41558-020-00952-0

Palmer, T. N. (2000). Predicting uncertainty in forecasts of weather and climate. *Reports on Progress in Physics*, *63*(2), 71.

Pathak, R., Dasari, H. P., Ashok, K., & Hoteit, I. (2023). Effects of multi-observations uncertainty and models similarity on climate change projections. *Npj Climate and Atmospheric Science*, *6*(1), 144.

Pradhan, P., Shrestha, S., Sundaram, S. M., & Virdis, S. G. (2021). Evaluation of the CMIP5 general circulation models for simulating the precipitation and temperature of the Koshi River Basin in Nepal. *Journal of Water and Climate Change*, *12*(7), 3282–3296.

Ren, X., Li, L., Yu, Y., Xiong, Z., Yang, S., Du, W., & Ren, M. (2020). A simplified climate change model and extreme weather model based on a machine learning method. *Symmetry*, *12*(1), 139.

Riahi, K., Van Vuuren, D. P., Kriegler, E., Edmonds, J., O'neill, B. C., Fujimori, S., Bauer, N., Calvin, K., Dellink, R., & Fricko, O. (2017). The Shared Socioeconomic Pathways and their energy, land use, and greenhouse gas emissions implications: An overview. *Global Environmental Change*, *42*, 153–168.

Roberts, M. J., Vidale, P. L., Senior, C., Hewitt, H. T., Bates, C., Berthou, S., Chang, P., Christensen, H. M., Danilov, S., & Demory, M.-E. (2018). The benefits of global high resolution for climate simulation: Process understanding and the enabling of stakeholder decisions at the regional scale. *Bulletin of the American Meteorological Society*, *99*(11), 2341–2359.

Seo, S. B., Kim, Y.-O., Kim, Y., & Eum, H.-I. (2019). Selecting climate change scenarios for regional hydrologic impact studies based on climate extremes indices. *Climate Dynamics*, *52*(3–4), 1595–1611. https://doi.org/10.1007/s00382-018-4210-7

Shiogama, H., Abe, M., & Tatebe, H. (2019). MIROC MIROC6 model output prepared for CMIP6 ScenarioMIP ssp245. *(No Title)*. https://cir.nii.ac.jp/crid/1880302168201969792

Shrestha, M., Acharya, S. C., & Shrestha, P. K. (2017). Bias correction of climate models for hydrological modelling – are simple methods still useful? *Meteorological Applications*, *24*(3), 531–539. https://doi.org/10.1002/met.1655

Sillmann, J., Kharin, V. V., Zhang, X., Zwiers, F. W., & Bronaugh, D. (2013). Climate extremes indices in the CMIP5 multimodel ensemble: Part 1. Model evaluation in the present climate. *Journal of Geophysical Research: Atmospheres*, *118*(4), 1716–1733. https://doi.org/10.1002/jgrd.50203

Srivastava, A., Grotjahn, R., & Ullrich, P. A. (2020). Evaluation of historical CMIP6 model simulations of extreme precipitation over contiguous US regions. *Weather and Climate Extremes*, *29*, 100268.

Sỳs, V., Fošumpaur, P., & Kašpar, T. (2021). The impact of climate change on the reliability of water resources. *Climate*, *9*(11), 153.

Teutschbein, C., & Seibert, J. (2012). Bias correction of regional climate model simulations for hydrological climate-change impact studies: Review and evaluation of different methods. *Journal of Hydrology*, *456*, 12–29.

Updated 30-year reference period reflects changing climate. (2021, May 5). World Meteorological Organization. https://public.wmo.int/media/news/updated-30-year-reference-period-reflects-changing-climate

van Vuuren, D. P., Edmonds, J., Kainuma, M., Riahi, K., Thomson, A., Hibbard, K., Hurtt, G. C., Kram, T., Krey, V., Lamarque, J.-F., Masui, T., Meinshausen, M., Nakicenovic, N., Smith, S. J., & Rose, S. K. (2011). The representative concentration pathways: An overview. *Climatic Change*, *109*(1), 5. https://doi.org/10.1007/s10584-011-0148-z

Van Vuuren, D. P., Edmonds, J., Kainuma, M., Riahi, K., Thomson, A., Hibbard, K., Hurtt, G. C., Kram, T., Krey, V., Lamarque, J.-F., Masui, T., Meinshausen, M., Nakicenovic, N., Smith, S. J., & Rose, S. K. (2011). The representative concentration pathways: An overview. *Climatic Change*, *109*(1–2), 5–31. https://doi.org/10.1007/s10584-011-0148-z

Volodin, E. M., Mortikov, E. V., Kostrykin, S. V., Galin, V. Ya., Lykossov, V. N., Gritsun, A. S., Diansky, N. A., Gusev, A. V., Iakovlev, N. G., Shestakova, A. A., & Emelina, S. V. (2018). Simulation of the modern climate using the INM-CM48 climate model. *Russian Journal of Numerical Analysis and Mathematical Modelling*, *33*(6), 367–374. https://doi.org/10.1515/rnam-2018-0032

Wang, F., & Tian, D. (2024). Multivariate bias correction and downscaling of climate models with trend-preserving deep learning. *Climate Dynamics*, *62*(10), 9651–9672. https://doi.org/10.1007/s00382-024-07406-9

Webster, M. D., & Sokolov, A. P. (1998). *Quantifying the uncertainty in climate predictions*. https://dspace.mit.edu/handle/1721.1/3610

Wehner, M. F., Smith, R. L., Bala, G., & Duffy, P. (2010). The effect of horizontal resolution on simulation of very extreme US precipitation events in a global atmosphere model. *Climate Dynamics*, *34*(2–3), 241–247. https://doi.org/10.1007/s00382-009-0656-y

Wieners, K.-H., Giorgetta, M., Jungclaus, J., Reick, C., Esch, M., Bittner, M., Legutke, S., Schupfner, M., Wachsmann, F., & Gayler, V. (2019). MPI-M MPI-ESM1. 2-HR model output prepared for CMIP6 CMIP amip. *(No Title)*. https://cir.nii.ac.jp/crid/1884242817203043200

Wijngaard, R. R., Herrington, A. R., Lipscomb, W. H., Leguy, G. R., & An, S.-I. (2023). Exploring the ability of the variable-resolution Community Earth System Model to simulate cryospheric–hydrological variables in High Mountain Asia. *The Cryosphere*, *17*(9), 3803–3828.

Yukimoto, S., Kawai, H., Koshiro, T., Oshima, N., Yoshida, K., Urakawa, S., Tsujino, H., Deushi, M., Tanaka, T., & Hosaka, M. (2019). The Meteorological Research Institute Earth System Model version 2.0, MRI-ESM2. 0: Description and basic evaluation of the physical component. *Journal of the Meteorological Society of Japan. Ser. II*, *97*(5), 931–965.

Zelinka, M. D., Myers, T. A., McCoy, D. T., Po-Chedley, S., Caldwell, P. M., Ceppi, P., Klein, S. A., & Taylor, K. E. (2020). Causes of Higher Climate Sensitivity in CMIP6

Models. *Geophysical Research Letters*, *47*(1), e2019GL085782. https://doi.org/10.1029/2019GL085782

Zhao, M., & Boll, J. (2022). Adaptation of water resources management under climate change. *Frontiers in Water*, *4*, 983228.

त्रिभुवन विश्वविद्यालय
Tribhuvan University
इन्जिनियरिङ्ग अध्ययन संस्थान
Institute of Engineering
थापाथली क्याम्पस
THAPATHALI CAMPUS
Accredited By University Grants Commission (UGC) Nepal, 2024

GPO Box- 280, Thapathali, Kathmandu
Tel: 01-5339766
E-mail: info@tcioe.edu.np
Website: www.tcioe.edu.np
गोश्वारा पो. नं. २८०, थापाथली, काठमाडौं
फोन: ०१-५३३५७६६

Date: April 21, 2025

To Whom It May Concern:

This is to certify that the paper titled **"Ranking and Evaluation of CMIP6 Climate Models Using Extreme Climate Indices: Application to the Seti Gandaki River Basin"** (Submission# **476**) submitted by **susmita khanal** as the first author, which had been accepted for presentation after the peer-review process, has successfully been presented at the 16th IOE Graduate Conference held during April 18 - 20, 2025. Kindly note that the final revision of the papers and publication process of the conference proceedings is still underway and hence inclusion of the accepted manuscript in the conference proceedings is contingent upon timely response to further edits during the publication process.

INSTITUTE OF ENGINEERING
16th IOE Graduate Conference, 2025
THAPATHALI CAMPUS

Dr. Raj Kumar Chaulagain,
Convener,
16th IOE Graduate Conference

079MSCCD018_Susmitakhanal_Thesisreport (1).pdf

Tribhuvan University

Document Details

Submission ID
trn:oid:::3117:455471084

Submission Date
May 4, 2025, 2:14 PM GMT+5:45

Download Date
May 4, 2025, 2:48 PM GMT+5:45

File Name
079MSCCD018_Susmitakhanal_Thesisreport (1).pdf

File Size
2.0 MB

84 Pages

22,729 Words

129,794 Characters

7% Overall Similarity

The combined total of all matches, including overlapping sources, for each database.

Filtered from the Report

- Bibliography
- Quoted Text
- Small Matches (less than 10 words)

Match Groups

91 Not Cited or Quoted 7%
Matches with neither in-text citation nor quotation marks

3 Missing Quotations 0%
Matches that are still very similar to source material

0 Missing Citation 0%
Matches that have quotation marks, but no in-text citation

0 Cited and Quoted 0%
Matches with in-text citation present, but no quotation marks

Top Sources

6% Internet sources
5% Publications
0% Submitted works (Student Papers)

Integrity Flags

1 Integrity Flag for Review

Replaced Characters
343 suspect characters on 53 pages
Letters are swapped with similar characters from another alphabet.

Our system's algorithms look deeply at a document for any inconsistencies that would set it apart from a normal submission. If we notice something strange, we flag it for you to review.

A Flag is not necessarily an indicator of a problem. However, we'd recommend you focus your attention there for further review.

Match Groups

- **91** Not Cited or Quoted 7%
  Matches with neither in-text citation nor quotation marks
- **3** Missing Quotations 0%
  Matches that are still very similar to source material
- **0** Missing Citation 0%
  Matches that have quotation marks, but no in-text citation
- **0** Cited and Quoted 0%
  Matches with in-text citation present, but no quotation marks

Top Sources

6% Internet sources
5% Publications
0% Submitted works (Student Papers)

Top Sources

The sources with the highest number of matches within the submission. Overlapping sources will not be displayed.

1	Internet	
elibrary.tucl.edu.np		1%
2	Internet	
conference.ioe.edu.np		1%
3	Internet	
repository.buc.ac.ke:8080		<1%
4	Publication	
Muhammad Shakeel, Hussnain Abbas, Ayesha Waseem, Zulfiqar Ali. "Adaptive en...		<1%
5	Internet	
iwaponline.com		<1%
6	Publication	
Pragya Pradhan, Sangam Shrestha, S. Mohana Sundaram, Salvatore G. P. Virdis. "...		<1%
7	Publication	
Temesgen Gashaw, Abeyou W. Worqlul, Meron Teferi Taye, Haileyesus Belay Lake...		<1%
8	Publication	
Pir Mohammad, Qihao Weng. "Asian heat stress variations in a changing climate: ...		<1%
9	Publication	
Mikhael G. Alemu, Melsew A. Wubneh, Dejene Sahlu, Fasikaw A. Zimale. "Spatiote...		<1%
10	Internet	
link.springer.com		<1%

11 Internet
www.researchgate.net <1%

12 Internet
books.aosis.co.za <1%

13 Publication
Kevin M. Grise, Mitchell K. Kelleher. "Midlatitude Cloud Radiative Effect Sensitivity... <1%

14 Internet
community.connective-cities.net <1%

15 Internet
espace.curtin.edu.au <1%

16 Publication
Triambak Baghel, Mukand S. Babel, Sangam Shrestha, Krishna Salin, Salvatore G.... <1%

17 Internet
flipkarma.com <1%

18 Internet
www.mdpi.com <1%

19 Internet
wcd.copernicus.org <1%

20 Internet
files.library.northwestern.edu <1%

21 Internet
journal.agrimetassociation.org <1%

22 Publication
Sanjiv Neupane, Sangam Shrestha, Usha Ghimire, S. Mohanasundaram, Sarawut ... <1%

23 Publication
Bowden, Christopher S.. "Improving Understanding of Climate Risks to Rice Prod... <1%

24 Internet
d197for5662m48.cloudfront.net <1%

25 Internet
earth-perspectives.springeropen.com <1%

26 Internet
elibrary.tucl.edu.np:8080 <1%

27 Internet
hdl.handle.net <1%

28 Internet
skepticalscience.com <1%

29 Internet
stax.strath.ac.uk <1%

30 Publication
Arnold Sullivan, Wenxiu Zhong, Gian Luca Eusebi Borzelli, Tao Geng et al. "Genera... <1%

31 Publication
Glauber Willian de Souza Ferreira, M. S. Reboita, J. G. M. Ribeiro, V. S. B. Carvalho ... <1%

32 Publication
Shella I. Talampas, Sangam Shrestha. "Watershed vulnerability assessment in the... <1%

33 Publication
Zulfaqar Sa'adi, Mohammad Saleh Al-Suwaiyan, Zaher Mundher Yaseen, Mou Leo... <1%

34 Internet
nora.nerc.ac.uk <1%

35 Publication
Jacob Agyekum, Thompson Annor, Emmanuel Quansah, Benjamin Lamptey, Leon... <1%

36 Publication
Jiafeng Liu, Yaqiong Lu. "How Well Do CMIP6 Models Simulate the Greening of th... <1%

37 Publication
Junaid Maqsood, Hassan Afzaal, Aitazaz A. Farooque, Farhat Abbas, Xander Wang,... <1%

38 Publication
Ramesh Chhetri, Vishnu P. Pandey, Rocky Talchabhadel, Bhesh Raj Thapa. "How d... <1%

39 Publication

Samit Thapa, Bo Li, Donglei Fu, Xiaofei Shi, Bo Tang, Hong Qi, Kun Wang. "Trend a... <1%

40 Publication

Suresh Raj Subedi, Manoj Lamichhane, Susan Dhungana, Bibek Chalise, Shishir B... <1%

41 Internet

centaur.reading.ac.uk <1%